



NSF Engineering Research Center for  
Computer Integrated Surgical Systems and  
Technology



LABORATORY FOR  
**Computational  
Sensing + Robotics**  
THE JOHNS HOPKINS UNIVERSITY


## Registration – Part 2

### 600.455/655 Computer Integrated Surgery



**WHITING  
SCHOOL OF  
ENGINEERING**  
THE JOHNS HOPKINS UNIVERSITY

**Russell H. Taylor**  
John C. Malone Professor of Computer Science,  
with joint appointments in Mechanical Engineering, Radiology & Surgery  
Director, Laboratory for Computational Sensing and Robotics  
The Johns Hopkins University  
[rht@jhu.edu](mailto:rht@jhu.edu)



1

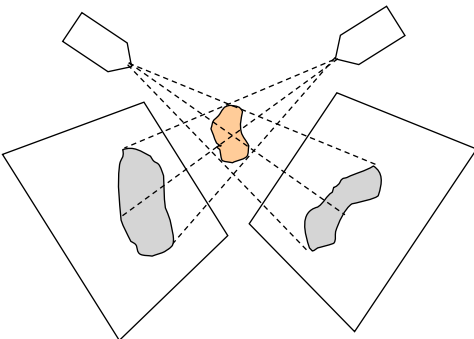
## Feature-Based 2D-3D Registration

**Given**

- 3D surface model of an anatomic structure
- Multiple 2D x-ray projection images taken at known poses relative to some coordinate system C
- Initial estimate of the pose **F** of the anatomic object relative to the x-ray imaging coordinate system C


**Goal**

- Compute an accurate value for **F**

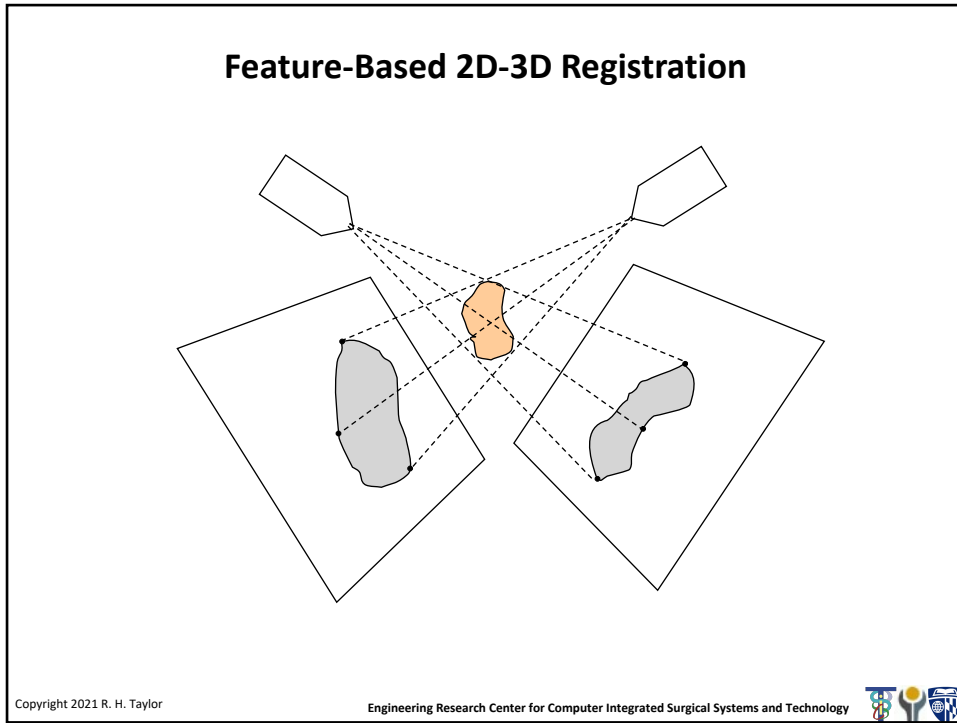


Copyright 2021 R. H. Taylor

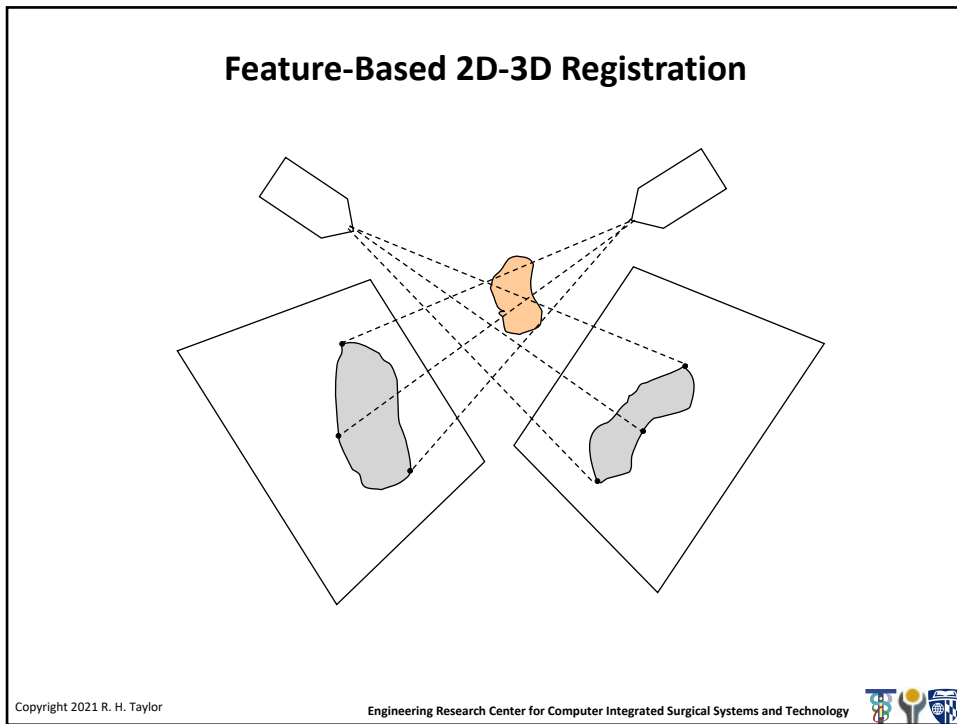
Engineering Research Center for Computer Integrated Surgical Systems and Technology



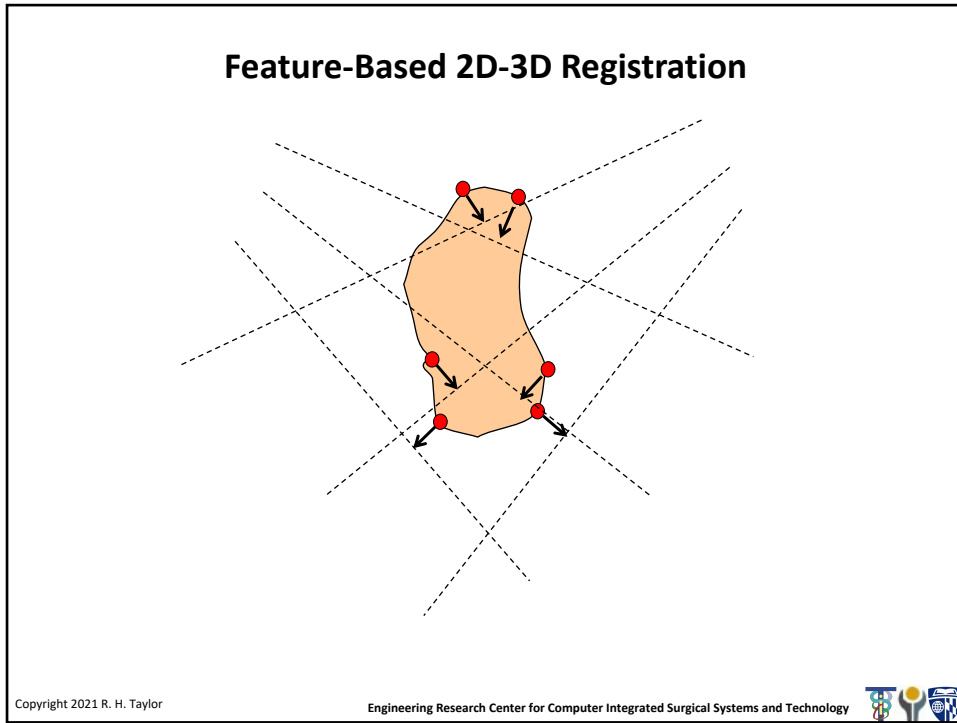
2



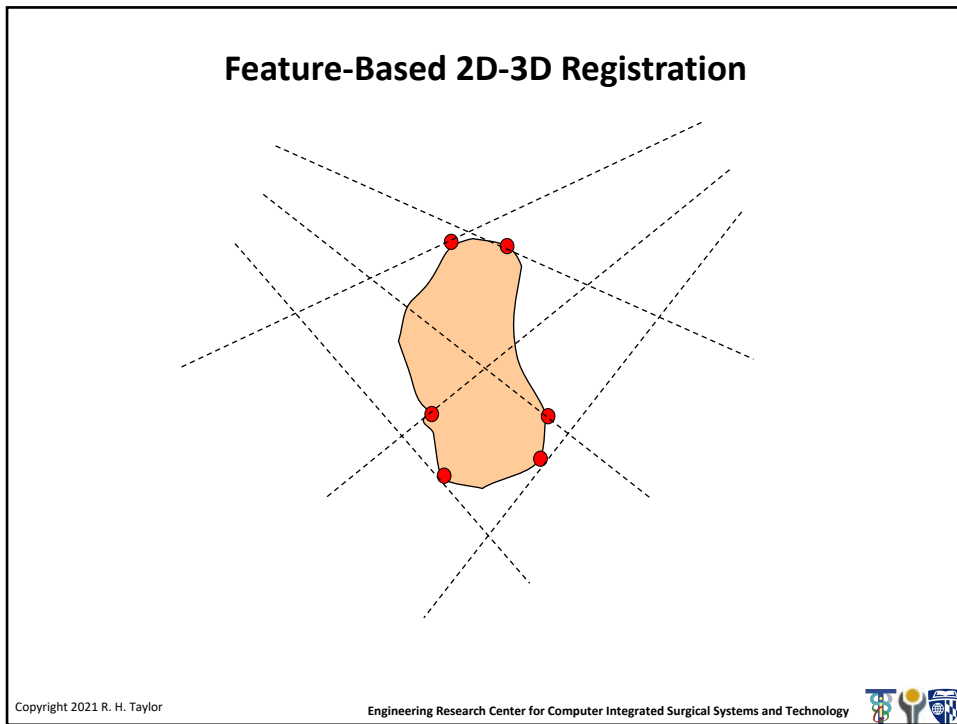
3



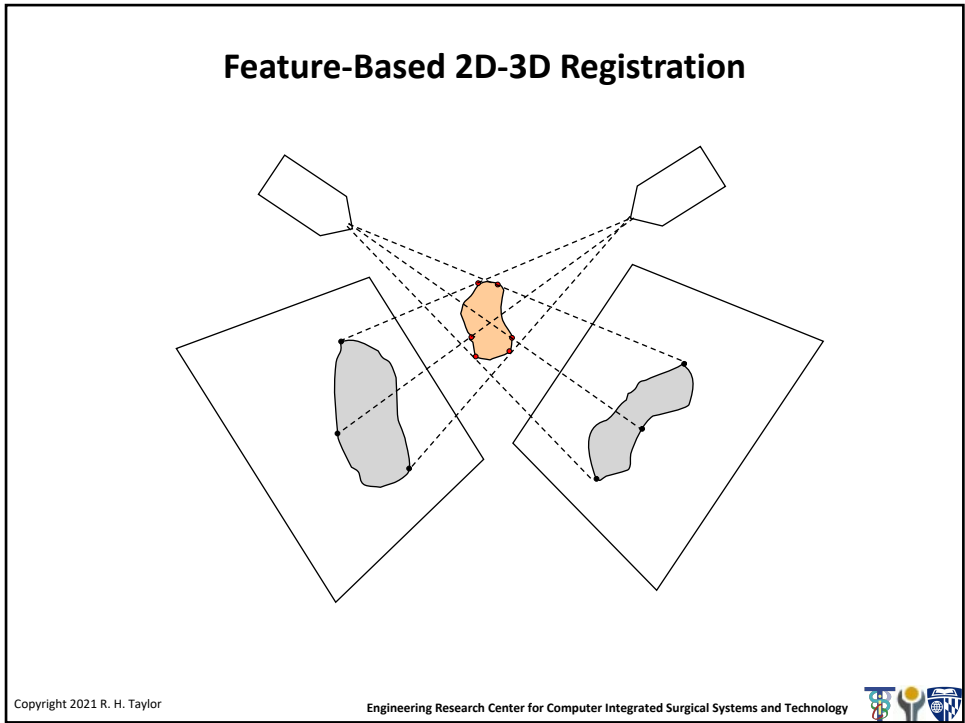
4



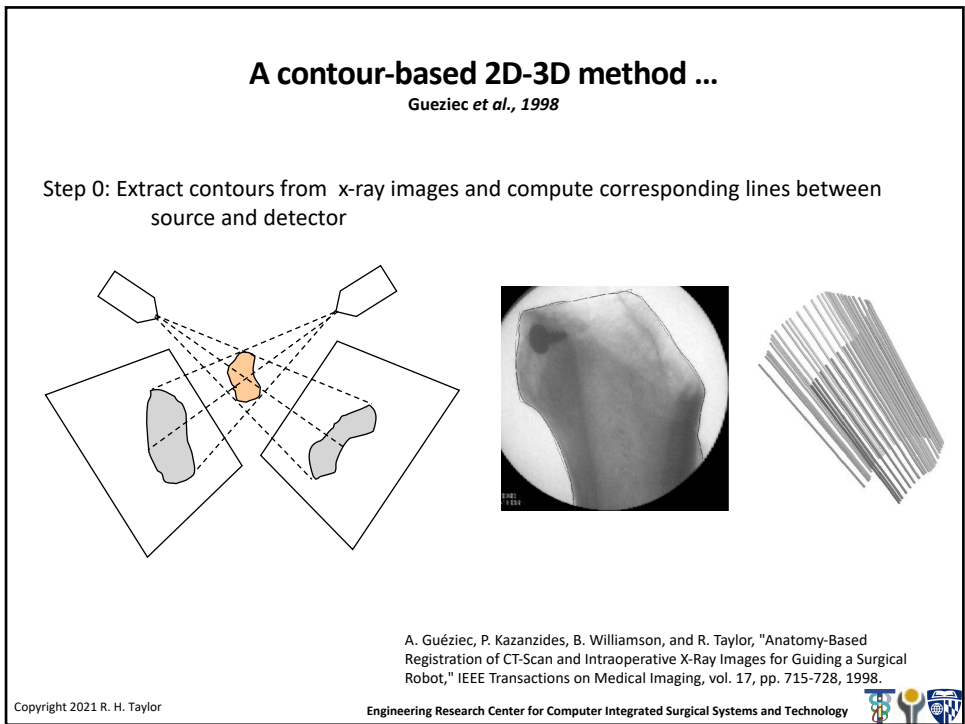
5



6



7

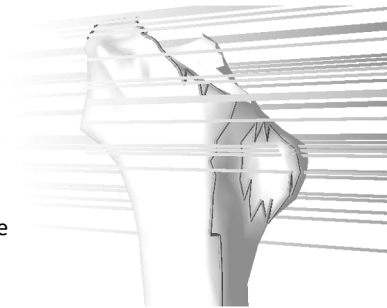


8

### A contour-based 2D-3D method ...

Guezic *et al.*, 1998

- Step 1: Given the current estimate for  $F = [R, t]$ , compute the apparent projection contours of the model for each viewing direction.
- Step 2: For each x-ray path line  $L_i$ , identify the closest point  $p_i$  on an apparent projection contour. This will give a set of points on the body surface to be moved toward the corresponding x-ray lines



A. Guéziec, P. Kazanzides, B. Williamson, and R. Taylor, "Anatomy-Based Registration of CT-Scan and Intraoperative X-Ray Images for Guiding a Surgical Robot," IEEE Transactions on Medical Imaging, vol. 17, pp. 715-728, 1998.

Copyright 2021 R. H. Taylor

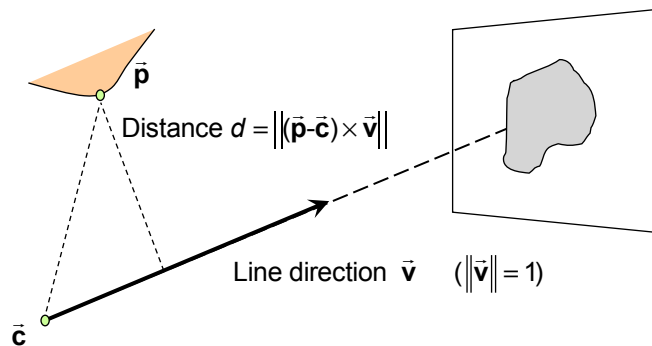
Engineering Research Center for Computer Integrated Surgical Systems and Technology



9

### A contour-based 2D-3D method ...

Guezic *et al.*, 1998



Note: It is convenient to use the x-ray source position (i.e., the center of convergence for a bundle of x-ray projection lines) as the value for  $\bar{c}$ .

A. Guéziec, P. Kazanzides, B. Williamson, and R. Taylor, "Anatomy-Based Registration of CT-Scan and Intraoperative X-Ray Images for Guiding a Surgical Robot," IEEE Transactions on Medical Imaging, vol. 17, pp. 715-728, 1998.

Copyright 2021 R. H. Taylor

Engineering Research Center for Computer Integrated Surgical Systems and Technology

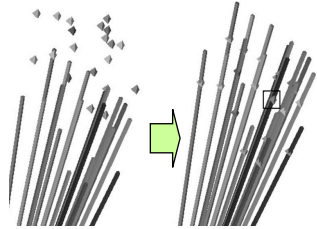


10

### A contour-based 2D-3D method ...

Guezic et al., 1998

Step 3: Solve an optimization problem to compute a value of  $F$  that minimizes the distance between the  $p_i$  and the  $L_i$ .



$$\min_{\mathbf{R}, \mathbf{t}} \sum_i d_i^2 = \min_{\mathbf{R}, \mathbf{t}} \sum_i \left\| \bar{\mathbf{v}}_i \times (\mathbf{c}_i - (\mathbf{R}\bar{\mathbf{p}}_i + \bar{\mathbf{t}})) \right\|^2$$

$$= \min_{\mathbf{R}, \mathbf{t}} \sum_i \left\| \text{skew}(\bar{\mathbf{v}}_i) \bullet (\mathbf{c}_i - (\mathbf{R}\bar{\mathbf{p}}_i + \bar{\mathbf{t}})) \right\|^2$$

Step 4: Iterate steps 1-3 until reach convergence

A. Guézic, P. Kazanzides, B. Williamson, and R. Taylor, "Anatomy-Based Registration of CT-Scan and Intraoperative X-Ray Images for Guiding a Surgical Robot," IEEE Transactions on Medical Imaging, vol. 17, pp. 715-728, 1998.

Copyright 2021 R. H. Taylor

Engineering Research Center for Computer Integrated Surgical Systems and Technology



11

### Computational Note

Guezic uses the Cayley parameterization for rotations:

$$\mathbf{R}(\bar{\mathbf{u}}) = (\mathbf{I} - \text{skew}(\bar{\mathbf{u}}))(\mathbf{I} + \text{skew}(\bar{\mathbf{u}}))^{-1}$$

This leads to the approximation

$$\mathbf{R}(\bar{\mathbf{u}}) \approx \mathbf{I} + \text{skew}(2\bar{\mathbf{u}})$$

which is similar to our familiar  $\mathbf{R}(\bar{\alpha}) \approx \mathbf{I} + \text{skew}(\bar{\alpha})$ .

He also uses the notation  $\mathbf{U} = \text{skew}(\bar{\mathbf{u}})$ . So  $\mathbf{R}(\bar{\mathbf{u}}) = (\mathbf{I} - \mathbf{U})(\mathbf{I} + \mathbf{U})^{-1}$

Similarly, we will see  $\mathbf{V} = \text{skew}(\bar{\mathbf{v}})$ , etc.

Copyright 2021 R. H. Taylor

Engineering Research Center for Computer Integrated Surgical Systems and Technology



12

### A contour-based 2D-3D method ...

Guezic et al., 1998

Guezic compared three different methods for performing the minimization in Step 3:

- Levenberg Marquardt (LM) nonlinear minimization.
- Linearization and constrained minimization
- Use of a Robust M-Estimator

A. Guéziec, P. Kazanzides, B. Williamson, and R. Taylor, "Anatomy-Based Registration of CT-Scan and Intraoperative X-Ray Images for Guiding a Surgical Robot," IEEE Transactions on Medical Imaging, vol. 17, pp. 715-728, 1998.

Copyright 2021 R. H. Taylor

Engineering Research Center for Computer Integrated Surgical Systems and Technology



13

### Levenberg-Marquardt ...

(Following development in Guezic et al., 1998)

Define  $f_i(\vec{x}) = \|\mathbf{V}_i(\vec{c}_i - \mathbf{R}(\vec{u})\vec{p}_i - \vec{t})\|$  where  $\vec{x}^t = [\vec{u}^t, \vec{t}^t]$ ,  $\mathbf{V}_i = \text{skew}(\vec{v}_i)$

Our goal is to minimize

$$\varepsilon(\vec{x}) = \sum_i f_i(\vec{x})^2 = \sum_i \|\mathbf{V}_i(\vec{c}_i - \mathbf{R}(\vec{u})\vec{p}_i - \vec{t})\|^2$$

We note that  $\varepsilon(\vec{x})$  is nonlinear. Levenberg-Marquardt is a widely used optimization method for problems of this type. However, it requires us to evaluate the partial derivatives  $\partial f_i / \partial x_j$ . Guezic worked these out symbolically for his problem

A. Guéziec, P. Kazanzides, B. Williamson, and R. Taylor, "Anatomy-Based Registration of CT-Scan and Intraoperative X-Ray Images for Guiding a Surgical Robot," IEEE Transactions on Medical Imaging, vol. 17, pp. 715-728, 1998.

Copyright 2021 R. H. Taylor

Engineering Research Center for Computer Integrated Surgical Systems and Technology



14

### Levenberg-Marquardt ...

(Following development in Guezic et al., 1998)

Define  $f_i(\bar{x}) = \|\mathbf{V}_i(\bar{\mathbf{c}}_i - \mathbf{R}(\bar{\mathbf{u}})\bar{\mathbf{p}}_i - \bar{\mathbf{t}})\|$  where  $\bar{x}^t = [\bar{\mathbf{u}}^t, \bar{\mathbf{t}}^t]$ ,  $\mathbf{V}_i = \text{skew}(\bar{\mathbf{v}}_i)$

$$\mathbf{J} = \begin{bmatrix} \dots & \frac{\partial f_i}{\partial \bar{x}} & \dots \end{bmatrix} = \begin{bmatrix} \dots & \frac{\partial f_i}{\partial \bar{\mathbf{u}}} & \dots \\ \dots & \frac{\partial f_i}{\partial \bar{\mathbf{t}}} & \dots \end{bmatrix}$$

$$\frac{\partial f_i}{\partial \bar{\mathbf{t}}} = \frac{\mathbf{V}_i^t \mathbf{V}_i (\mathbf{R}\bar{\mathbf{p}}_i - \mathbf{c} + \bar{\mathbf{t}})}{f_i}$$

$$\frac{\partial f_i}{\partial \bar{\mathbf{u}}} = \left( \frac{\partial \mathbf{R}\bar{\mathbf{p}}_i}{\partial \bar{\mathbf{u}}} \right)^t \frac{\mathbf{V}_i^t \mathbf{V}_i (\mathbf{R}\bar{\mathbf{p}}_i - \mathbf{c} + \bar{\mathbf{t}})}{f_i}$$

Details on this may be found  
in reference [45] of  
Guezic's paper

A. Guéziec, P. Kazanzides, B. Williamson, and R. Taylor, "Anatomy-Based Registration of CT-Scan and Intraoperative X-Ray Images for Guiding a Surgical Robot," IEEE Transactions on Medical Imaging, vol. 17, pp. 715-728, 1998.

Copyright 2021 R. H. Taylor

Engineering Research Center for Computer Integrated Surgical Systems and Technology



15

### Levenberg-Marquardt ...

(Following development in Guezic et al., 1998)

Step 1: Pick  $\lambda =$  a small number; pick initial guess for  $\bar{x}$

Step 2: Evaluate  $f_i(\bar{x})$  and  $\mathbf{J}$  and solve the least squares problem

$$\begin{bmatrix} \vdots \\ (\mathbf{J}^t \mathbf{J} + \lambda \mathbf{I}) \Delta \bar{x} - \mathbf{J}^t f_i \\ \vdots \end{bmatrix} = \begin{bmatrix} \vdots \\ 0 \\ \vdots \end{bmatrix}$$

for  $\Delta \bar{x}$ .

Step 3:  $\bar{x} \leftarrow \bar{x} + \Delta \bar{x}$ ; update  $\lambda$ .

Step 4: Evaluate termination condition. If not done, go back to step 2

Note: Usually  $\lambda$  starts small and grows larger. Consult standard references (e.g., Numerical Recipes) for more information.

A. Guéziec, P. Kazanzides, B. Williamson, and R. Taylor, "Anatomy-Based Registration of CT-Scan and Intraoperative X-Ray Images for Guiding a Surgical Robot," IEEE Transactions on Medical Imaging, vol. 17, pp. 715-728, 1998.

Copyright 2021 R. H. Taylor

Engineering Research Center for Computer Integrated Surgical Systems and Technology



16



### Constrained Linearized Least Squares ...

(Following development in Guezic et al., 1998)

Step 0: Make an initial guess for  $\mathbf{R}$  and  $\bar{\mathbf{t}}$

Step 1: Compute  $\bar{\mathbf{p}}_i \leftarrow \mathbf{R}\mathbf{p}_i + \bar{\mathbf{t}}$

Step 2: Define  $\mathbf{P}_i = \text{skew}(\bar{\mathbf{p}}_i)$ ,  $\mathbf{V}_i = \text{skew}(\bar{\mathbf{v}}_i)$

Step 3: Solve the least squares problem:

$$\varepsilon^2 = \min \left\| \begin{bmatrix} \vdots & \vdots \\ 2\mathbf{V}\mathbf{P}_i & \mathbf{V}_i \\ \vdots & \vdots \end{bmatrix} \begin{bmatrix} \bar{\mathbf{u}} \\ \Delta\bar{\mathbf{t}} \end{bmatrix} - \begin{bmatrix} \vdots \\ \mathbf{V}_i(\bar{\mathbf{c}}_i - \bar{\mathbf{p}}_i) \\ \vdots \end{bmatrix} \right\|^2 \quad \text{subject to } \|\bar{\mathbf{u}}\| \leq \rho$$

where  $\rho$  is sufficiently small so that  $\mathbf{I} + 2\mathbf{U}$  approximates a rotation

Step 4: Compute  $\Delta\mathbf{R} = (\mathbf{I} - \mathbf{U})(\mathbf{I} + \mathbf{U})^{-1}$

Update  $\mathbf{p}_i \leftarrow \Delta\mathbf{R}\mathbf{p}_i + \Delta\bar{\mathbf{t}}$ ;  $\mathbf{R} \leftarrow \Delta\mathbf{R}\mathbf{R}$ ;  $\bar{\mathbf{t}} \leftarrow \Delta\mathbf{R}\bar{\mathbf{t}} + \Delta\bar{\mathbf{t}}$

Step 5: If  $\varepsilon$  is small enough or some other termination condition is met, then stop. Otherwise go back to Step 2.

A. Guéziec, P. Kazanzides, B. Williamson, and R. Taylor, "Anatomy-Based Registration of CT-Scan and Intraoperative X-Ray Images for Guiding a Surgical Robot," IEEE Transactions on Medical Imaging, vol. 17, pp. 715-728, 1998.

Copyright 2021 R. H. Taylor

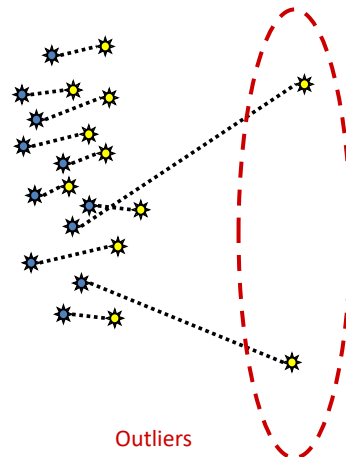
Engineering Research Center for Computer Integrated Surgical Systems and Technology



17

### Robust Pose Estimation ...

- Basic idea is to identify outliers and give them little or no weight.



R. Kumar and A. R. Hanson, "Robust methods for estimating pose and a sensitivity analysis," Comput. Vision, Graphics, Image Processing-IV, vol. 60, no. 3, pp. 313-342, 1994.

Copyright 2021 R. H. Taylor

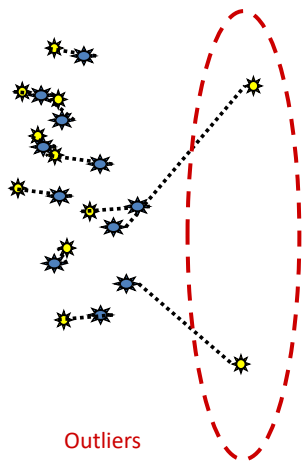
Engineering Research Center for Computer Integrated Surgical Systems and Technology



18


### Robust Pose Estimation ...

- Basic idea is to identify outliers and give them little or no weight.



Outliers

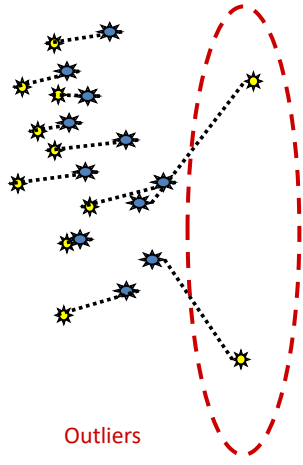
R. Kumar and A. R. Hanson, "Robust methods for estimating pose and a sensitivity analysis," *Comput. Vision, Graphics, Image Processing-1U*, vol. 60, no. 3, pp. 313–342, 1994.

Copyright 2021 R. H. Taylor Engineering Research Center for Computer Integrated Surgical Systems and Technology 

19


### Robust Pose Estimation ...

- Basic idea is to identify outliers and give them little or no weight.



Outliers

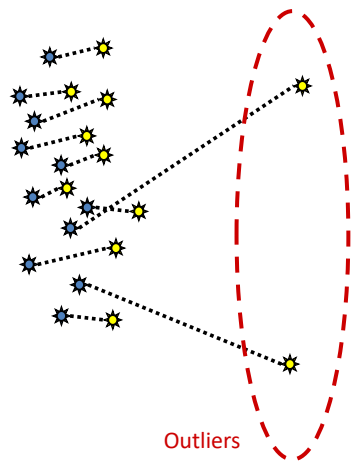
R. Kumar and A. R. Hanson, "Robust methods for estimating pose and a sensitivity analysis," *Comput. Vision, Graphics, Image Processing-1U*, vol. 60, no. 3, pp. 313–342, 1994.

Copyright 2021 R. H. Taylor Engineering Research Center for Computer Integrated Surgical Systems and Technology 

20


### Robust Pose Estimation ...

- Basic idea is to identify outliers and give them little or no weight.



Outliers

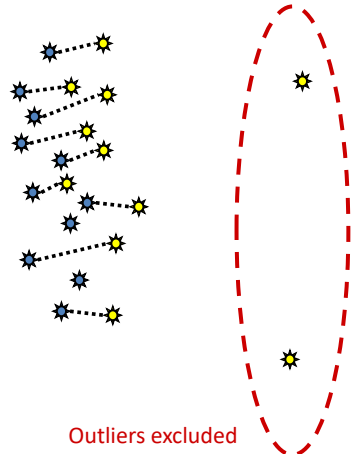
R. Kumar and A. R. Hanson, "Robust methods for estimating pose and a sensitivity analysis," *Comput. Vision, Graphics, Image Processing-IU*, vol. 60, no. 3, pp. 313–342, 1994.

Copyright 2021 R. H. Taylor Engineering Research Center for Computer Integrated Surgical Systems and Technology 

21


### Robust Pose Estimation ...

- Basic idea is to identify outliers and give them little or no weight.



Outliers excluded

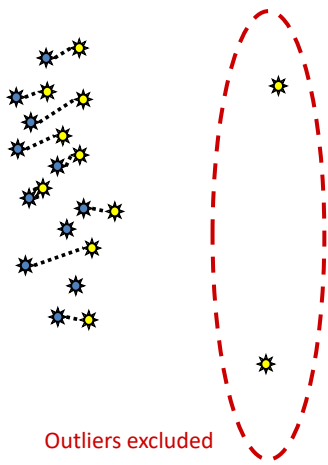
R. Kumar and A. R. Hanson, "Robust methods for estimating pose and a sensitivity analysis," *Comput. Vision, Graphics, Image Processing-IU*, vol. 60, no. 3, pp. 313–342, 1994.

Copyright 2021 R. H. Taylor Engineering Research Center for Computer Integrated Surgical Systems and Technology 

22


### Robust Pose Estimation ...

- Basic idea is to identify outliers and give them little or no weight.



Outliers excluded

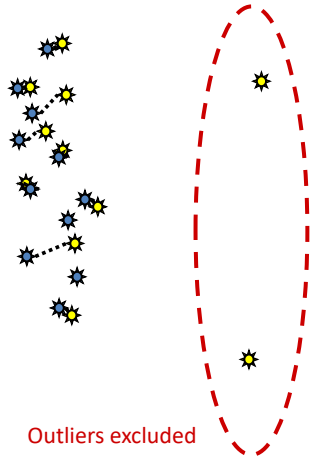
R. Kumar and A. R. Hanson, "Robust methods for estimating pose and a sensitivity analysis," *Comput. Vision, Graphics, Image Processing-IU*, vol. 60, no. 3, pp. 313–342, 1994.

Copyright 2021 R. H. Taylor Engineering Research Center for Computer Integrated Surgical Systems and Technology 

23


### Robust Pose Estimation ...

- Basic idea is to identify outliers and give them little or no weight.



Outliers excluded

R. Kumar and A. R. Hanson, "Robust methods for estimating pose and a sensitivity analysis," *Comput. Vision, Graphics, Image Processing-IU*, vol. 60, no. 3, pp. 313–342, 1994.

Copyright 2021 R. H. Taylor Engineering Research Center for Computer Integrated Surgical Systems and Technology 

24

### Robust M-Estimator ...

(Following development in Guezic et al., 1998)

Step 0: Make an initial guess for  $\mathbf{R}$  and  $\bar{\mathbf{t}}$

Step 1: Compute  $\bar{\mathbf{p}}_i \leftarrow \mathbf{R}\bar{\mathbf{p}}_i + \bar{\mathbf{t}}$

Step 2: Define  $\mathbf{P}_i = \text{skew}(\bar{\mathbf{p}}_i)$ ,  $\mathbf{V}_i = \text{skew}(\bar{\mathbf{v}}_i)$ ,

Step 3: Solve a robust linearized problem

$$\varepsilon = \arg \min_{\bar{\mathbf{u}}, \Delta \bar{\mathbf{t}}} \sum_i \rho \left( \frac{0.6745 e_i}{\text{median}(\{e_i\})} \right) \quad \text{where } e_i = \|\mathbf{V}_i(\bar{\mathbf{p}}_i - \mathbf{c}_i + 2\mathbf{P}_i\bar{\mathbf{u}} + \Delta \bar{\mathbf{t}})\|$$

(See next slide)

Step 4: Compute  $\Delta \mathbf{R} = (\mathbf{I} - \mathbf{U})(\mathbf{I} + \mathbf{U})^{-1}$

Update  $\mathbf{p}_i \leftarrow \Delta \mathbf{R}\mathbf{p}_i + \Delta \bar{\mathbf{t}}$ ;  $\mathbf{R} \leftarrow \Delta \mathbf{R}\mathbf{R}$ ;  $\bar{\mathbf{t}} \leftarrow \Delta \mathbf{R}\bar{\mathbf{t}} + \Delta \bar{\mathbf{t}}$

Step 5: If  $\varepsilon$  is small enough or some other termination condition is met, then stop. Otherwise go back to Step 2.

A. Guéziec, P. Kazanzides, B. Williamson, and R. Taylor, "Anatomy-Based Registration of CT-Scan and Intraoperative X-Ray Images for Guiding a Surgical Robot," IEEE Transactions on Medical Imaging, vol. 17, pp. 715-728, 1998.

Copyright 2021 R. H. Taylor

Engineering Research Center for Computer Integrated Surgical Systems and Technology



25

### Robust M-Estimator ...

(Following development in Guezic et al., 1998)

Step 3.0: Set  $\bar{\mathbf{u}} = \bar{\mathbf{0}}$ ,  $\Delta \bar{\mathbf{t}} = \bar{\mathbf{0}}$

Step 3.1: Compute  $e_i = \|\mathbf{V}_i(\bar{\mathbf{p}}_i - \bar{\mathbf{c}}_i + 2\mathbf{P}_i\bar{\mathbf{u}} + \Delta \bar{\mathbf{t}})\|$ ,  $s = \text{median}(\{\dots, e_i, \dots\}) / 0.6745$ ,

Step 3.2: Solve  $\mathbf{C}\bar{\mathbf{x}} = \bar{\mathbf{d}}$ , where  $\bar{\mathbf{x}}^t = [\bar{\mathbf{u}}^t, \bar{\mathbf{t}}^t]$

$$\mathbf{C} = \sum_i \Psi \left( \frac{e_i}{s} \right) \begin{bmatrix} 2\mathbf{P}_i\mathbf{W}_i\mathbf{P}_i & \mathbf{P}_i\mathbf{W}_i \\ 2\mathbf{P}_i\mathbf{W}_i & \mathbf{W}_i \end{bmatrix} \quad \text{and} \quad \bar{\mathbf{d}} = \sum_i \Psi \left( \frac{e_i}{s} \right) \begin{bmatrix} \mathbf{P}_i\mathbf{W}_i(\bar{\mathbf{c}}_i - \bar{\mathbf{p}}_i) \\ \mathbf{W}_i(\bar{\mathbf{c}}_i - \bar{\mathbf{p}}_i) \end{bmatrix}$$

$$\text{where } \mathbf{W}_i = \mathbf{V}_i^t \mathbf{V}_i = \mathbf{I} - \bar{\mathbf{v}}_i \bar{\mathbf{v}}_i^t \quad \Psi(\mu) = \begin{cases} \mu(1 - \mu^2 / \alpha^2)^2 & \text{if } \|\mu\| \leq \alpha \\ 0 & \text{otherwise} \end{cases}$$

(Note: We use  $\alpha=2$ )

Step 3.3: Iterate steps 3.1 and 3.2 until a suitable termination condition is reached.

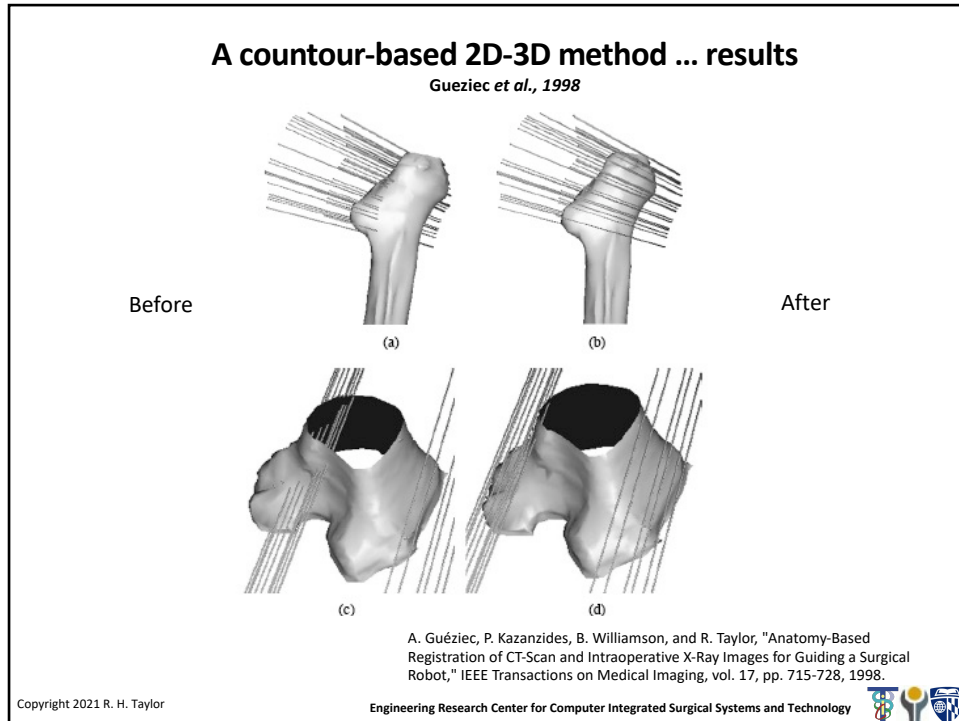
A. Guéziec, P. Kazanzides, B. Williamson, and R. Taylor, "Anatomy-Based Registration of CT-Scan and Intraoperative X-Ray Images for Guiding a Surgical Robot," IEEE Transactions on Medical Imaging, vol. 17, pp. 715-728, 1998.

Copyright 2021 R. H. Taylor

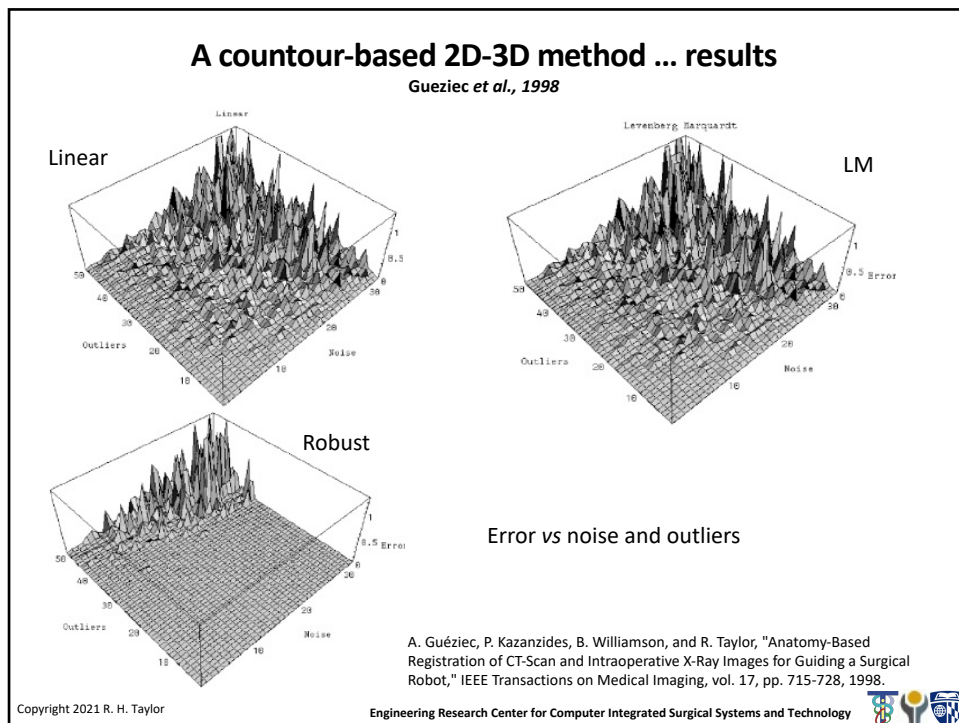
Engineering Research Center for Computer Integrated Surgical Systems and Technology



26



27



28

## A contour-based 2D-3D method ... times

Gueziec *et al.*, 1998

TABLE I  
AVERAGE EXECUTION TIMES IN MS FOR THE THREE  
REGISTRATION METHODS APPLIED TO DATA SETS THAT  
COMPRISE 100 POINTS (TOP) AND 20 POINTS (BOTTOM)

| Number Points/Method  | LM  | Linear | Robust |
|-----------------------|-----|--------|--------|
| 100 points (CPU time) | 790 | 690    | 28     |
| 20 points (CPU time)  | 200 | 42     | 9.6    |

A. Guéziec, P. Kazanzides, B. Williamson, and R. Taylor, "Anatomy-Based Registration of CT-Scan and Intraoperative X-Ray Images for Guiding a Surgical Robot," IEEE Transactions on Medical Imaging, vol. 17, pp. 715-728, 1998.

Copyright 2021 R. H. Taylor

Engineering Research Center for Computer Integrated Surgical Systems and Technology



29

## Sample Set Analysis

- **Question:** How good is a particular set of 3D sample points for the purpose of registration to a 3D surface?
- Long line of authors have looked at this question
- Next few slides are based on the work of David Simon, et al (1995)

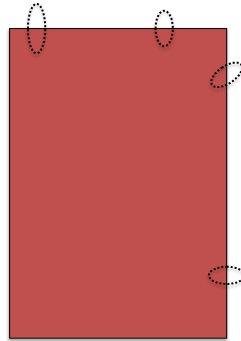
Copyright 2021 R. H. Taylor

Engineering Research Center for Computer Integrated Surgical Systems and Technology



33

## Sample Set Selection



Copyright 2021 R. H. Taylor

Engineering Research Center for Computer Integrated Surgical Systems and Technology



34

## Sample Set Analysis: Distance Estimates

Let

$$F(\mathbf{x}) = 0$$

be the implicit equation of a surface, then one good estimate of the distance of a point  $\mathbf{x}$  to the surface is

$$D(\mathbf{x}) = \frac{F(\mathbf{x})}{\|\nabla F(\mathbf{x})\|}$$

Copyright 2021 R. H. Taylor

Engineering Research Center for Computer Integrated Surgical Systems and Technology



35



### Sample set analysis: sensitivity

Let  $\mathbf{x}_s$  be a point on the surface, and let  $T(\bar{\eta})$  represent a small perturbation with parameters  $\bar{\eta}$  with respect to the surface of point  $\mathbf{x}_s$ :

$$\mathbf{x}'_s = T(\bar{\eta})\mathbf{x}_s$$

Then we define  $\mathbf{V}(\mathbf{x}_s)$  to be

$$\mathbf{V}(\mathbf{x}_s) = \frac{\partial D(T(\bar{\eta})\mathbf{x}_s)}{\partial \bar{\eta}} = \begin{bmatrix} \mathbf{n}_s \\ \mathbf{x}_s \times \mathbf{n}_s \end{bmatrix}$$

where  $\mathbf{n}_s$  is the unit normal to the surface at  $\mathbf{x}_s$ . So,

$$D(T(\bar{\eta})\mathbf{x}_s) \simeq \mathbf{V}^T(\mathbf{x}_s)\bar{\eta}$$

Squaring this gives

$$\begin{aligned} D^2(T(\bar{\eta})\mathbf{x}_s) &\simeq \bar{\eta}^T \mathbf{V}(\mathbf{x}_s) \mathbf{V}^T(\mathbf{x}_s) \bar{\eta} \\ &= \bar{\eta}^T \mathbf{M}(\mathbf{x}_s) \bar{\eta} \end{aligned}$$

Note that  $\mathbf{M}$  is  $6 \times 6$  positive, semi-definite, symmetric matrix.

Copyright 2021 R. H. Taylor

Engineering Research Center for Computer Integrated Surgical Systems and Technology



36

### Sample set analysis: sensitivity

For a region  $\mathcal{R}$ , define

$$\begin{aligned} E_R(\bar{\eta}) &= \bar{\eta}^T \left[ \sum_{\mathbf{x}_s \in \mathcal{R}} \mathbf{M}(\mathbf{x}_s) \right] \bar{\eta} \\ &= \bar{\eta}^T \Psi_{\mathcal{R}} \bar{\eta} \\ &= \bar{\eta}^T \mathbf{Q} \Lambda \mathbf{Q}^T \bar{\eta} \\ &= \sum_{1 \leq i \leq 6} \lambda_i (\bar{\eta}^T \cdot \mathbf{q}_i)^2 \end{aligned}$$

- Note that the eigenvectors  $\mathbf{q}_i$  correspond to small differential transformations  $\mathbf{T}(\mathbf{q}_i)$ , and can sort eigenvalues so that

$$\lambda_1 \geq \lambda_2 \geq \dots \geq \lambda_6$$

- Note that eigenvector  $\mathbf{q}_1$  corresponds to direction of greatest constraint.
- Similarly, can also think of  $\mathbf{q}_6$  as the least constrained direction.

Copyright 2021 R. H. Taylor

chnology



37

### Sample Set Analysis: Goodness Measures

- Magnitude of smallest eigenvalue (Simon)
- (Kim and Khosla)

$$\frac{\sqrt[6]{\lambda_1 \cdot \dots \cdot \lambda_6}}{\lambda_1 + \dots + \lambda_6}$$

- Nahvi

$$\frac{\lambda_6^2}{\lambda_1}$$

Copyright 2021 R. H. Taylor

Engineering Research Center for Computer Integrated Surgical Systems and Technology



38

### Sample Set Selection

- One blind search method (similar to Simon, 1995) is:
  - Randomly select sample points on surface
  - (prune for reachability)
  - evaluate goodness of sample set using some criterion
  - repeat many times and choose the best one found

Copyright 2021 R. H. Taylor

Engineering Research Center for Computer Integrated Surgical Systems and Technology



39

## Sample Set Selection

- Refinement of blind search (hill climbing):
  - Randomly select sample points on surface
  - (prune for reachability)
  - evaluate goodness of sample set using some criterion
  - replace a point from sample set with a randomly selected point
  - evaluate goodness
  - if better, keep it
  - else revert to original point and try again
- Variations include simulated annealing, “genetic” algorithms

Copyright 2021 R. H. Taylor

Engineering Research Center for Computer Integrated Surgical Systems and Technology



40

## Sample Set Selection: Another Alternative

- Select large number of random points  $\mathbf{x}_s$
- Prune for reachability
- For each point, compute constraint direction  $\mathbf{V}_s = \mathbf{V}(\mathbf{x}_s)$ . To a first approximation, a measurement at  $\mathbf{x}_s$  with accuracy  $\epsilon_s$  constrains  $\bar{\eta}$  by

$$|\mathbf{V}_s \bar{\eta}| \leq \epsilon_s$$

- Now select subset of the  $\mathbf{x}_s$  that minimizes, e.g.,

$$\min_{\delta_s} \max \bar{\eta}^T \mathbf{S} \bar{\eta}$$

subject to

$$\begin{aligned} \delta_s &\in \{0, 1\} \\ |\delta_s \mathbf{V}_s \bar{\eta}| &\leq \epsilon_s \\ \sum_s \delta_s &\leq \text{subsetsize} \end{aligned}$$

There are various ways to do this.

Copyright 2021 R. H. Taylor

Engineering Research Center for Computer Integrated Surgical Systems and Technology



41

## Sample Set Selection: Another Alternative (con'd)

- One can also minimize other forms, e.g.,

$$\min_s \max_i |\sigma_i \eta_i|$$

subject to similar constraints

- An alternative is to minimize the number of sample points required to ensure that some constraints on  $\bar{\eta}$  are guaranteed to be met. E.g.,

$$\min_{\delta_s} \sum \delta_s$$

such that

$$\delta_s \in \{0, 1\}$$

$$\xi \leq \xi_{limit}$$

where

$$\xi = \max_{\bar{\eta}} \bar{\eta}^T \mathbf{S} \bar{\eta}$$

or some other form subject to

$$|\delta_s \mathbf{V}_s \bar{\eta}| \leq \epsilon_s$$

Copyright 2021 R. H. Taylor

Engineering Research Center for Computer Integrated Surgical Systems and Technology



42

## Probabilistic Registration

- Registration methods typically use some optimization algorithm to find a “best” transformation between one data set and the other.
- It makes sense to try to find the “most likely” registration transformation.
- ICP minimizes sum-of-squares distances.
- This is equivalent to assuming that point-pair match probabilities are independent and symmetric Gaussian distributions based on distances
- But there are a number of other methods that explicitly consider probabilities ...

Copyright 2021 R. H. Taylor

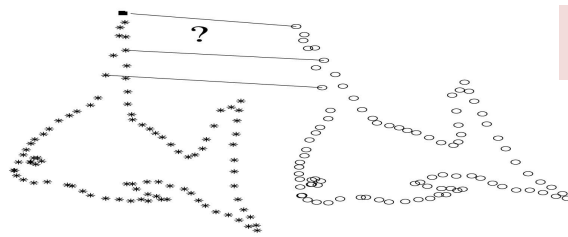
Engineering Research Center for Computer Integrated Surgical Systems and Technology



43

## Coherent Point Drift

- A. Myronenko and X. Song, "Point-Set Registration: Coherent Point Drift", *IEEE Trans. on Pattern Analysis and Machine Intelligence*, vol. 32- 12, pp. 2262-2275, 2010.
- Alignment of point clouds
  - Fast method follows "EM" paradigm
  - Tolerates outliers and noise
  - Transformations: Rigid, affine, general deformable



Click here  
for [slides](#)

Copyright 2021 R. H. Taylor

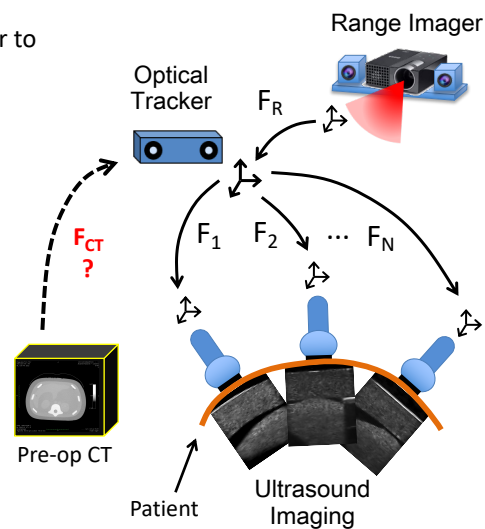
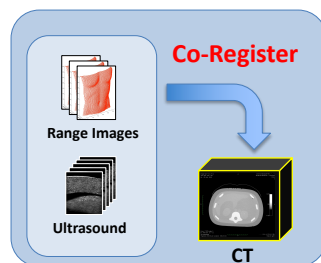
Engineering Research Center for Computer Integrated Surgical Systems and Technology



44

## Registration of intraoperative data to preoperative models

- Want to know registration from tracker to CT space
  - Provides tool positions relative to CT
- Data sources for registration
  - Tracked ultrasound
  - Tracked (or calibrated) range data



S. Billings and R. H. Taylor, "Iterative Most Likely Oriented Point Registration", in *Medical Image Computing and Computer-Assisted Interventions (MICCAI)*, Boston, October, 2014. (accepted).

Copyright 2021 R. H. Taylor

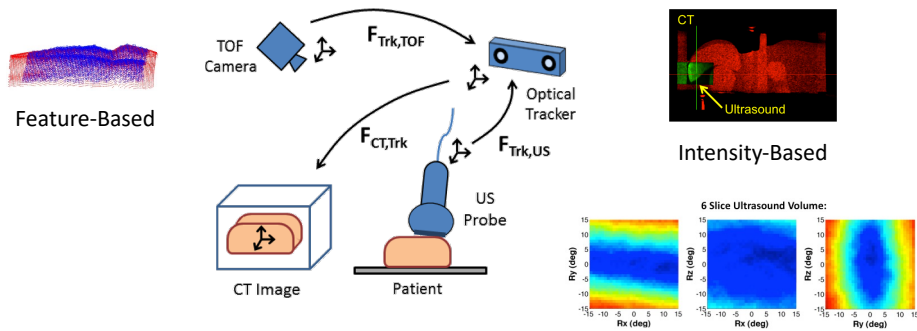
Engineering Research Center for Computer Integrated Surgical Systems and Technology



46

## Multi-Modal Feature-Based Registration

Question: How to combine multiple data sources, in order to improve the accuracy and robustness of registration outcomes?

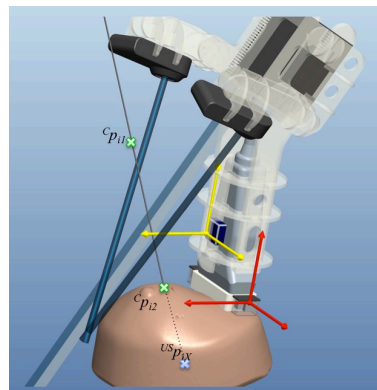


Billings S, Kapoor A, Keil M, Wood BJ, Boctor E (2011) A Hybrid Surface/Image-Based Approach to Facilitate Ultrasound/CT Registration. *SPIE, Medical Imaging 2011: Ultrasonic Imaging, Tomography, and Therapy* 7968: 79680V–79680V-12

47

## Example: Clear Guide Medical Navigation System

- Handheld device:
  - low cost
  - integrated on probe
  - ease of use
  - no workflow interruptions
  - in-situ guidance
  - no tool calibration
  - no sterility issues
  - high accuracy
  - real-time fusion
  - real-time quality control



Copyright 2021 R. H. Taylor

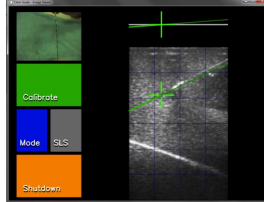
Engineering Research Center for Computer Integrated Surgical Systems and Technology



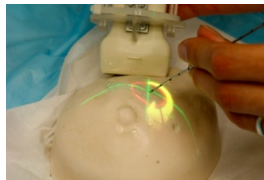
48

### Easy-to-Follow Guidance

- CG-1 has traditional ultrasound screen AND on-screen guidance overlay



- As well as on-patient projection



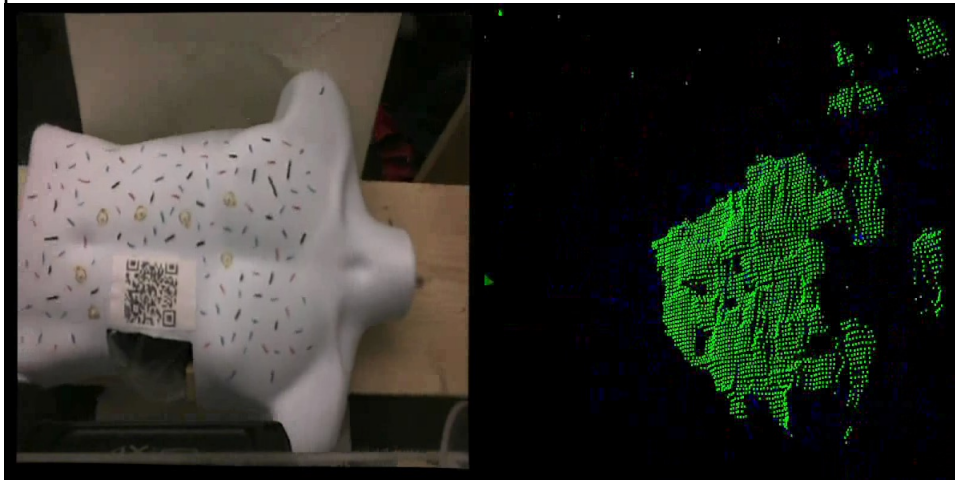
Copyright 2021 R. H. Taylor

Engineering Research Center for Computer Integrated Surgical Systems and Technology



49

### Real-time Multi-modal Fusion

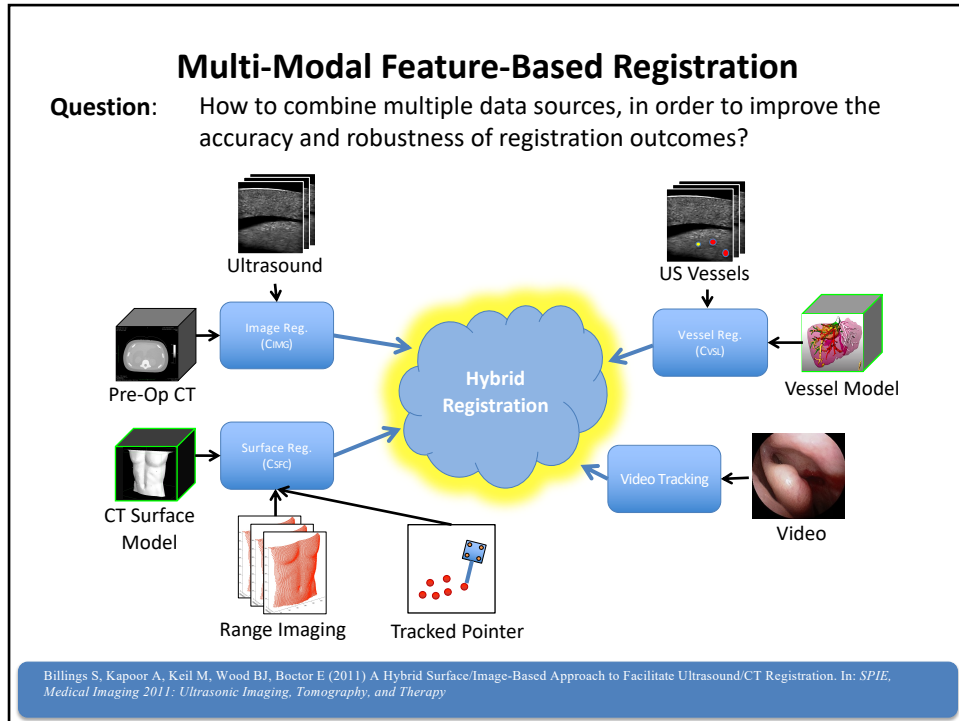


Copyright 2021 R. H. Taylor

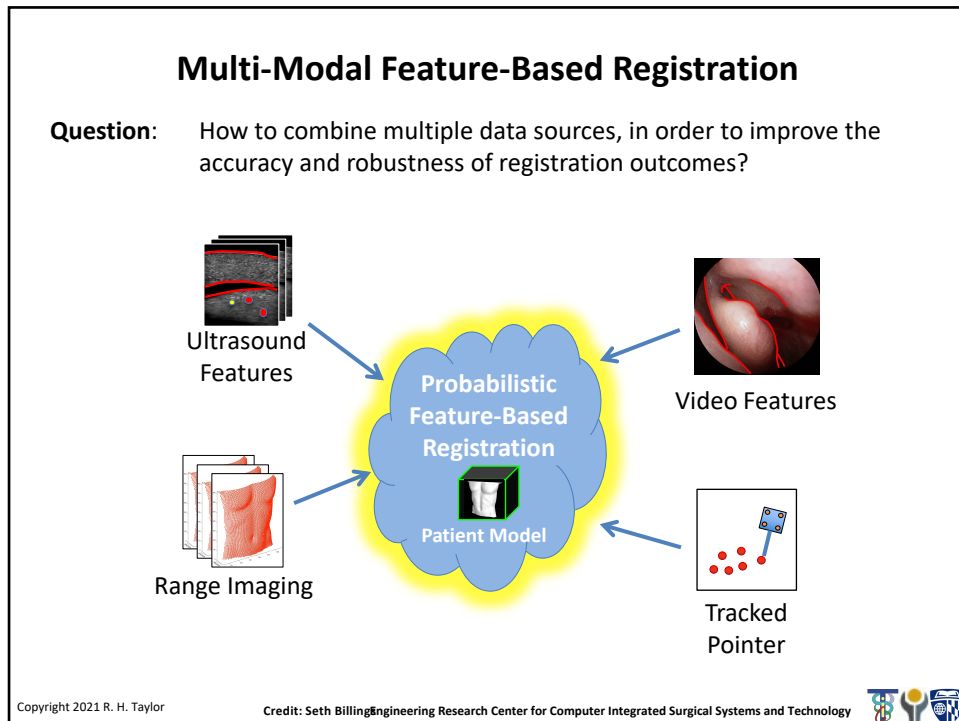
Engineering Research Center for Computer Integrated Surgical Systems and Technology



50



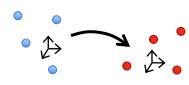
51



52



## Iterative Closest Point (ICP) Revisited



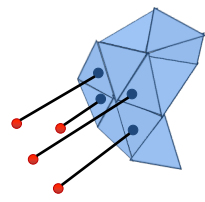
- Widely popular and useful method for point cloud to surface registration introduced by Besl & McKay in 1992
- Many variants proposed since its inception affecting all aspects of the algorithm (robustness, matching criteria, match alignment, etc.)

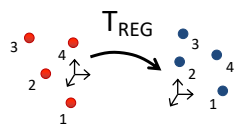
➤ **Matching Phase:**  
for each point in the source shape, find the closest point on the target shape

$$\mathbf{y}_i = C_{CP}(T(\mathbf{x}_i), \Psi) = \operatorname{argmin}_{\mathbf{y} \in \Psi} \|\mathbf{y} - T(\mathbf{x}_i)\|_2$$

➤ **Registration Phase:**  
compute transformation to minimize sum of square distances between matches

$$T = \operatorname{argmin}_T \sum_{i=1}^n \|\mathbf{y}_i - T(\mathbf{x}_i)\|_2^2$$





S. Billings and R. H. Taylor, "Iterative Most Likely Oriented Point Registration", in *Medical Image Computing and Computer-Assisted Interventions (MICCAI)*, Boston, October, 2014.  
 Copyright 2021 R. H. Taylor Credit: Seth Billing Engineering Research Center for Computer Integrated Surgical Systems and Technology

53

## Most-Likely Point Paradigm Illustrated with ICP

1. **Probability Model:** isotropic Gaussian
 
$$f_{\text{match}}(\mathbf{x} | \mathbf{y}, \sigma^2) = \frac{1}{(2\pi\sigma^2)^{3/2}} \cdot e^{-\frac{1}{2\sigma^2} \|\mathbf{y} - \mathbf{x}\|^2}$$
2. **Match Phase:**

$$\begin{aligned} \mathbf{y}_i &= \operatorname{argmax}_{\mathbf{y}_i \in \Psi} f_{\text{match}}(T(\mathbf{x}_i) | \mathbf{y}_i, \sigma^2) \\ &= \operatorname{argmax}_{\mathbf{y}_i \in \Psi} \frac{1}{(2\pi\sigma^2)^{3/2}} \cdot e^{-\frac{1}{2\sigma^2} \|\mathbf{y}_i - T(\mathbf{x}_i)\|^2} \\ &\rightarrow \operatorname{argmin}_{\mathbf{y}_i \in \Psi} \|\mathbf{y}_i - T(\mathbf{x}_i)\| \end{aligned}$$
3. **Registration Phase:**

$$\begin{aligned} \mathbf{T} &= \operatorname{argmax}_{\mathbf{T}} \prod_i^n f_{\text{match}}(T(\mathbf{x}_i) | \mathbf{y}_i, \sigma^2) \\ &= \operatorname{argmax}_{\mathbf{T}} \prod_i^n \frac{1}{(2\pi\sigma^2)^{3/2}} \cdot e^{-\frac{1}{2\sigma^2} \|\mathbf{y}_i - T(\mathbf{x}_i)\|^2} \\ &\rightarrow \operatorname{argmax}_{\mathbf{T}} \left[ -n \log \left( (2\pi\sigma^2)^{3/2} \right) - \frac{1}{2\sigma^2} \sum_i^n \|\mathbf{y}_i - T(\mathbf{x}_i)\|^2 \right] \\ &\rightarrow \operatorname{argmin}_{\mathbf{T}} \sum_i^n \|\mathbf{y}_i - T(\mathbf{x}_i)\|^2 \end{aligned}$$

Copyright 2021 R. H. Taylor Credit: Seth Billing Engineering Research Center for Computer Integrated Surgical Systems and Technology

54

### Outline of Registration Algorithms

- ICP - Iterative Closest Point
  - isotropic position data
- **IMLP - Iterative Most Likely Point**
  - anisotropic position data
  - robust to outliers
- IMLOP - Iterative Most Likely Oriented Point
  - isotropic position & orientation data
- G-IMLOP - Generalized IMLOP
  - anisotropic position & orientation data
- P-IMLOP - Projected IMLOP
  - anisotropic position & projected orientation data

Copyright 2021 R. H. Taylor Credit: Seth BillingEngineering Research Center for Computer Integrated Surgical Systems and Technology

56

### Sources of Anisotropic Uncertainty

#### Tomographic Imaging

#### Stereo Vision

#### Ultrasound

Figures: [http://www.ndigital.com/wp-content/uploads/2013/09/face\\_normals\\_v1.png](http://www.ndigital.com/wp-content/uploads/2013/09/face_normals_v1.png); The Essential Physics of Medical Imaging, 3rd Ed; [http://www.mhhe.com/engc/content/uploads/2013/01/L\\_A\\_8\\_Look-At-Baby-3D-Ultrasound-Tests-Ultrasound-Technicians-by-300x275.jpg](http://www.mhhe.com/engc/content/uploads/2013/01/L_A_8_Look-At-Baby-3D-Ultrasound-Tests-Ultrasound-Technicians-by-300x275.jpg); [http://001.lalimg.com/photo/v0/105832128/CT\\_Scan\\_equipment.jpg](http://001.lalimg.com/photo/v0/105832128/CT_Scan_equipment.jpg)

Copyright 2021 R. H. Taylor Credit: Seth BillingEngineering Research Center for Computer Integrated Surgical Systems and Technology

57

## Prior Work: Anisotropic Registration

- Generalized Total Least Squares ICP (GTLS-ICP)

Estépar RSJ, Brun A, Westin C-F (2004) Robust generalized total least squares iterative closest point registration. In: *MICCAI 2004*

- Registration Phase
  - anisotropic noise model
  - ad-hoc implementation **less accurate / efficient**; can be **unstable**
- Match Phase
  - isotropic (i.e. closest-point matching)

- Generalized ICP (G-ICP)

- Registration Phase
  - anisotropic noise model **limited** to model locally-linear surface regions surrounding each feature point of a point cloud shape
  - uses off-the-shelf conjugate gradient solver
- Match Phase
  - isotropic (i.e. closest-point matching)

Segal A, Haehnel D, Thrun S (2009) Generalized-ICP. In: *Robotics: Science and Systems V*

Copyright 2021 R. H. Taylor

Credit: Seth Billing Engineering Research Center for Computer Integrated Surgical Systems and Technology



58

## Prior Work: Anisotropic Registration

- Anisotropic ICP (A-ICP)

Maier-Hein L, Franz AM, Dos Santos TR, Schmidt M, Fangerau M, et al. (2012) Convergent iterative closest-point algorithm to accommodate anisotropic and inhomogeneous localization error. *IEEE Trans Pattern Anal Mach Intell* 34: 1520–1532.

- Registration Phase
  - anisotropic noise model
  - ad-hoc implementation **does not fully account** for noise in both shapes (i.e., lacks ability to reorient the data-shape covariances during optimization)
- Match Phase
  - anisotropic noise model with **non-optimal matching** (finds minimal Mahalanobis distance match rather than most-likely match)
  - **inefficient** implementation; also **cannot guarantee** that the “best” match is found
- **Initializes registration by ICP** (due to inefficient match phase)

Copyright 2021 R. H. Taylor

Credit: Seth Billings

Engineering Research Center for Computer Integrated Surgical Systems and Technology



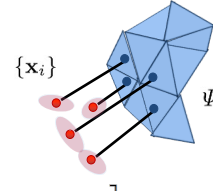
59

### Iterative Most Likely Point (IMLP)

**Probability Model:** anisotropic Gaussian

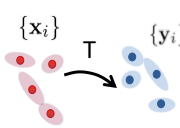
$$f_{\text{match}}(\mathbf{x} | \mathbf{y}, \Sigma_{\mathbf{x}}, \Sigma_{\mathbf{y}}) = \frac{1}{(2\pi)^{3/2} |\Sigma_{\mathbf{x}} + \Sigma_{\mathbf{y}}|^{1/2}} \cdot e^{-\frac{1}{2}(\mathbf{y}-\mathbf{x})^T (\Sigma_{\mathbf{x}} + \Sigma_{\mathbf{y}})^{-1} (\mathbf{y}-\mathbf{x})}$$

**Match Phase:**



$$[\mathbf{y}_i, \Sigma_{\mathbf{y}_i}] = \underset{[\mathbf{y}_i, \Sigma_{\mathbf{y}_i}] \in \Psi}{\text{argmin}} \left[ \log(\mathbf{R}\Sigma_{\mathbf{x}_i}\mathbf{R}^T + \Sigma_{\mathbf{y}_i}) + (\mathbf{y}_i - \mathbf{T}(\mathbf{x}_i))^T (\mathbf{R}\Sigma_{\mathbf{x}_i}\mathbf{R}^T + \Sigma_{\mathbf{y}_i})^{-1} (\mathbf{y}_i - \mathbf{T}(\mathbf{x}_i)) \right]$$

**Registration Phase:**

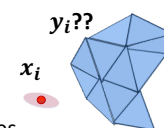


$$\mathbf{T} = \underset{\mathbf{T}=[\mathbf{R}, \mathbf{t}]}{\text{argmin}} \sum_i^n (\mathbf{y}_i - \mathbf{T}(\mathbf{x}_i))^T (\mathbf{R}\Sigma_{\mathbf{x}_i}\mathbf{R}^T + \Sigma_{\mathbf{y}_i})^{-1} (\mathbf{y}_i - \mathbf{T}(\mathbf{x}_i))$$

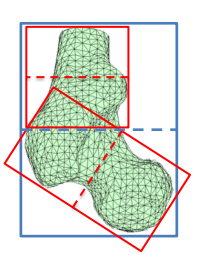
Billings SD, Boctor EM, Taylor RH (2015) Iterative Most-Likely Point Registration (IMLP): A Robust Algorithm for Computing Optimal Shape Alignment. *PLoS One* 10: e0117688

60

### IMLP: Match Phase



- Due to anisotropic distance metric, standard KD-tree search techniques do not apply.
- **Approach:** PD-tree search with modified node test



PD Tree Constructed by Datum Positions

**Constructing the PD tree:**

1. Add all datums to a root node
2. Compute covariance of datum positions within the node
3. Create minimally-sized bounding box aligned to the covariance eigenvectors
4. Partition node along the direction of greatest extent
5. Form left and right child nodes from the datums in each partition
6. Repeat from Step 2 for left and right child nodes until # datums in node < threshold or node size < threshold

Copyright 2021 R. H. Taylor      Credit: Seth Billings Engineering Research Center for Computer Integrated Surgical Systems and Technology

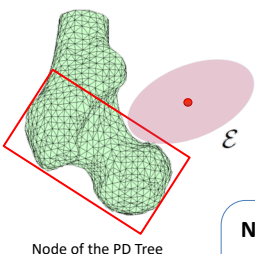
61

### IMLP: Match Phase

Searching the PD tree:

Assume the **current match candidate** has a match error equal to  $E_{best}$

**Question:** can any feature in this node possibly provide a match error less than  $E_{best}$ ?



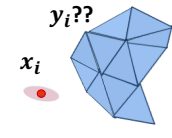
$$[y_i, \Sigma_{y_i}] = \underset{[y_i, \Sigma_{y_i}] \in \Psi}{\operatorname{argmin}} \left[ \log(\mathbf{R}\Sigma_{x_i}\mathbf{R}^T + \Sigma_{y_i}) + (y_i - T(x_i))^T (\mathbf{R}\Sigma_{x_i}\mathbf{R}^T + \Sigma_{y_i})^{-1} (y_i - T(x_i)) \right]$$

**True if:**  $(y_i - T(x_i))^T (\mathbf{R}\Sigma_{x_i}\mathbf{R}^T + \Sigma_{node})^{-1} (y_i - T(x_i)) < E_{best} - \log_{min}$

**Node Test:** if the **ellipsoid**

$$\mathcal{E} = \{y \mid (y - T(x_i))^T (\mathbf{R}\Sigma_{x_i}\mathbf{R}^T + \Sigma_{node})^{-1} (y - T(x_i)) \leq E_{best} - \log_{min}\}$$

intersects the bounding box of the node, then search the node



Copyright 2021 R. H. Taylor Credit: Seth Billings Engineering Research Center for Computer Integrated Surgical Systems and Technology

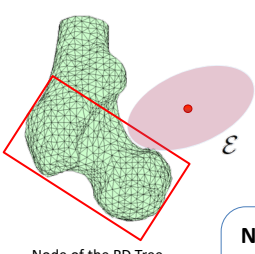
62

### IMLP: Match Phase

Searching the PD tree:

Assume the **current match candidate** has a match error equal to  $E_{best}$

**Question:** can any feature in this node possibly provide a match error less than  $E_{best}$ ?



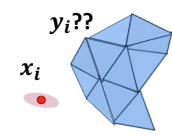
$$[y_i, \Sigma_{y_i}] = \underset{[y_i, \Sigma_{y_i}] \in \Psi}{\operatorname{argmin}} \left[ \log(\mathbf{R}\Sigma_{x_i}\mathbf{R}^T + \Sigma_{y_i}) + (y_i - T(x_i))^T (\mathbf{R}\Sigma_{x_i}\mathbf{R}^T + \Sigma_{y_i})^{-1} (y_i - T(x_i)) \right]$$

**True if:**  $(y_i - T(x_i))^T (\mathbf{R}\Sigma_{x_i}\mathbf{R}^T + \Sigma_{node})^{-1} (y_i - T(x_i)) < E_{best} - \log_{min}$

**Node Test:** if the **ellipsoid**

$$\mathcal{E} = \{y \mid (y - T(x_i))^T (\mathbf{R}\Sigma_{x_i}\mathbf{R}^T + \Sigma_{node})^{-1} (y - T(x_i)) \leq E_{best} - \log_{min}\}$$

intersects the bounding box of the node, then search the node

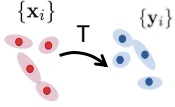


Details in Billings' Thesis

Copyright 2021 R. H. Taylor Credit: Seth Billings Engineering Research Center for Computer Integrated Surgical Systems and Technology

63

## IMLP: Registration Phase



1. Re-formulate the cost function from an unconstrained optimization

$$\mathbf{T} = \operatorname{argmin}_{[\mathbf{R}, \mathbf{t}]} \sum_{i=1}^n (\mathbf{y}_i - \mathbf{R}\mathbf{x}_i - \mathbf{t})^T (\mathbf{R}\Sigma_{x_i}\mathbf{R}^T + \Sigma_{y_i})^{-1} (\mathbf{y}_i - \mathbf{R}\mathbf{x}_i - \mathbf{t})$$

to a constrained optimization

$$\mathbf{T} = \operatorname{argmin}_{[\mathbf{R}, \mathbf{t}]} \sum_{i=1}^n (\mathbf{x}_i - \mathbf{x}_i^*)^T \Sigma_{x_i}^{-1} (\mathbf{x}_i - \mathbf{x}_i^*) + \sum_{i=1}^n (\mathbf{y}_i - \mathbf{y}_i^*)^T \Sigma_{y_i}^{-1} (\mathbf{y}_i - \mathbf{y}_i^*)$$

subject to:  $F_i(\mathbf{x}_i^*, \mathbf{y}_i^*, \mathbf{R}, \mathbf{t}) = \mathbf{y}_i^* - \mathbf{R}\mathbf{x}_i^* - \mathbf{t} = 0$  Generalized Total Least Squares (GTLS)

$\mathbf{x}_i^*$  - true (unknown) data-point position  
 $\mathbf{y}_i^*$  - true (unknown) model-point position

2. Linearize the constraints with a [Taylor series](#) centered at the measured (known) data

$$F_i(\mathbf{x}_i^*, \mathbf{y}_i^*, \mathbf{R}, \mathbf{t}) \approx F_{L,i}^k(\mathbf{x}_i, \mathbf{y}_i, \mathbf{d}\alpha, \mathbf{d}\mathbf{t})$$

$$= F_i^0(\mathbf{x}_i, \mathbf{y}_i, \mathbf{R}_k, \mathbf{t}_k) - \mathbf{r}_{y_i} + \mathbf{R}_k \mathbf{r}_{x_i} + \operatorname{skew}(\mathbf{R}_k \mathbf{x}_i) \mathbf{d}\alpha - \mathbf{d}\mathbf{t} = 0$$

Note using:  $\Delta \mathbf{R} \approx \mathbf{I} + \operatorname{skew}(\mathbf{d}\alpha)$      $\mathbf{r}_{x_i} = \mathbf{x}_i - \mathbf{x}_i^*$      $\mathbf{r}_{y_i} = \mathbf{y}_i - \mathbf{y}_i^*$

Copyright 2021 R. H. Taylor Credit: Seth Billing Engineering Research Center for Computer Integrated Surgical Systems and Technology

64

## IMLP: Registration Phase

3. Apply the method of [Lagrange multipliers](#) to solve constrained optimization.

3a. Form the [Lagrange function](#) using the linearized constraints

$$\mathcal{L}(\mathbf{d}\alpha, \mathbf{d}\mathbf{t}, \lambda) = \sum_{i=1}^n \mathbf{r}_{x_i}^T \Sigma_{x_i}^{-1} \mathbf{r}_{x_i} + \sum_{i=1}^n \mathbf{r}_{y_i}^T \Sigma_{y_i}^{-1} \mathbf{r}_{y_i} + \sum_{i=1}^n \lambda_i^T F_{L,i}^k(\mathbf{x}_i, \mathbf{y}_i, \mathbf{d}\alpha, \mathbf{d}\mathbf{t})$$

3b. Solve zero gradient w.r.t. the optimization parameters and the Lagrange multipliers

$$\mathbf{J}^T \Sigma^{-1} \mathbf{J} \mathbf{d}\mathbf{p} = -\mathbf{J}^T \Sigma^{-1} \mathbf{f}^0 \quad \text{modified Gauss-Newton}$$

$\mathbf{d}\mathbf{p} = \begin{bmatrix} \mathbf{d}\alpha \\ \mathbf{d}\mathbf{t} \end{bmatrix}$

$\mathbf{f}^0 = \begin{bmatrix} \mathbf{f}_1^0 \\ \vdots \\ \mathbf{f}_n^0 \end{bmatrix}$

$\mathbf{J} = \begin{bmatrix} \operatorname{skew}(\mathbf{R}_k \mathbf{x}_1) & -\mathbf{I} \\ \vdots & \vdots \\ \operatorname{skew}(\mathbf{R}_k \mathbf{x}_n) & -\mathbf{I} \end{bmatrix}$

$\Sigma = \begin{bmatrix} \mathbf{F}_x^0 \Sigma_x \mathbf{F}_x^{0T} + \Sigma_y \end{bmatrix}$

$\mathbf{F}_x^0 = \begin{bmatrix} -\mathbf{R}_k & & \\ & \ddots & \\ & & -\mathbf{R}_k \end{bmatrix}$

$\Sigma_x = \begin{bmatrix} \Sigma_{x1} & & \\ & \ddots & \\ & & \Sigma_{xn} \end{bmatrix}$

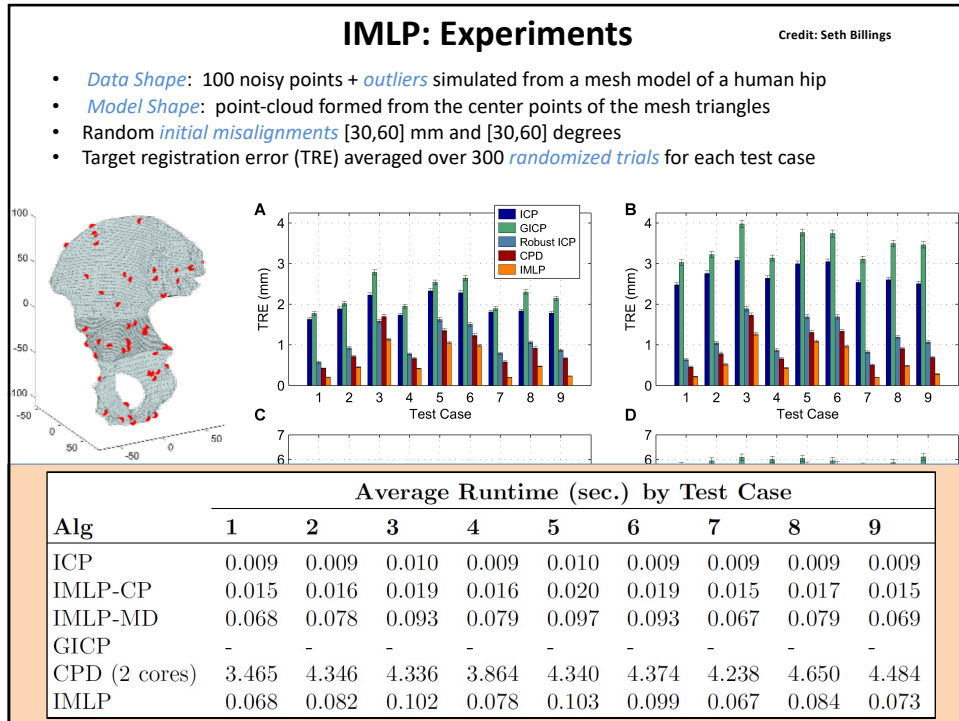
$\Sigma_y = \begin{bmatrix} \Sigma_{y1} & & \\ & \ddots & \\ & & \Sigma_{yn} \end{bmatrix}$

4. Iteratively solve 3b by linear least squares until convergence.

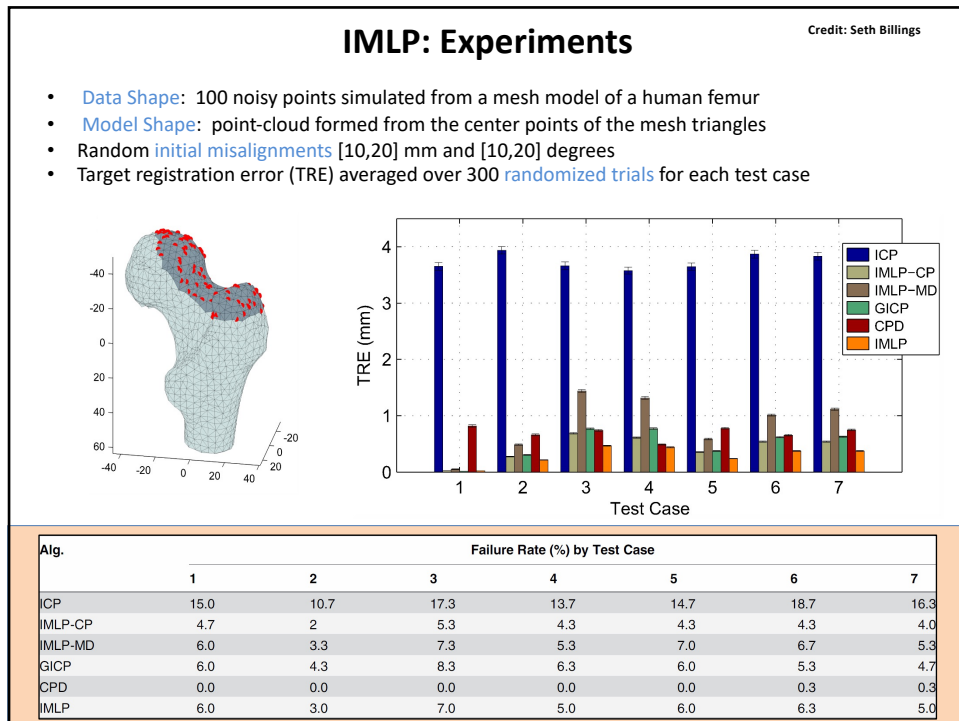
$$\mathbf{R}_{k+1} = \mathbf{R}(\mathbf{d}\alpha) \mathbf{R}_k, \quad \mathbf{t}_{k+1} = \mathbf{t}_k + \mathbf{d}\mathbf{t}$$

Copyright 2021 R. H. Taylor Credit: Seth Billing Engineering Research Center for Computer Integrated Surgical Systems and Technology

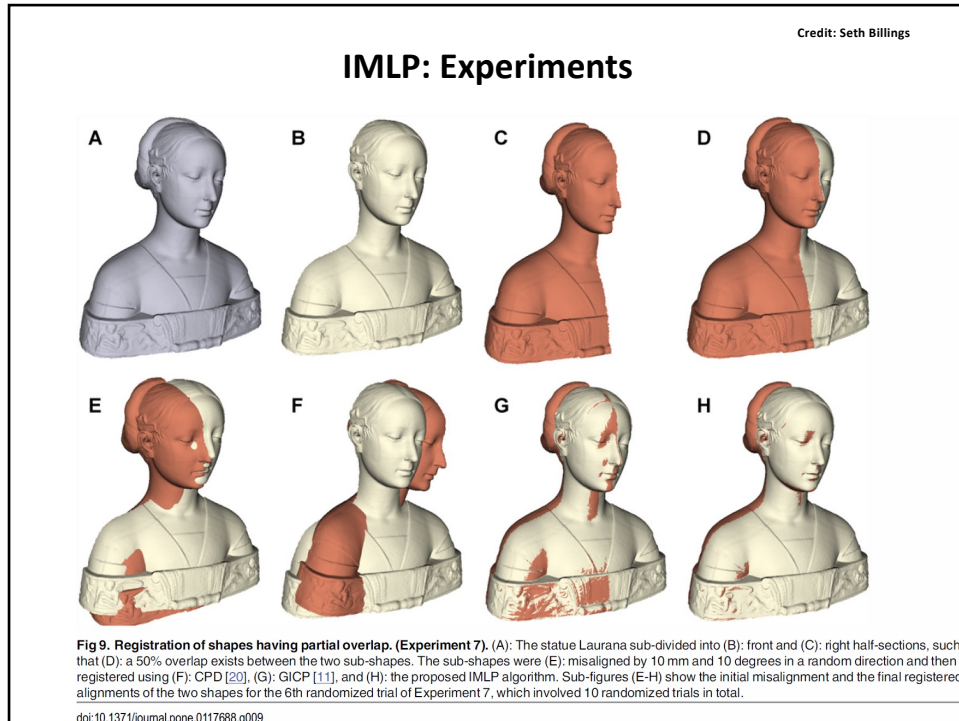
65



67



68



69

## Iterative Most Likely Oriented Point (IMLOP)

➤ **Matching Phase:**  
for each oriented point in the source shape, find the most likely oriented point on the target shape

$$y_i = C_{MLP}(T(x_i), \Psi) = \operatorname{argmax}_{y \in \Psi} f_{\text{match}}(T(x_i), y)$$

➤ **Registration Phase:**  
compute transformation to maximize the likelihood (i.e. minimize negative log-likelihood) of oriented point matches

$$T = \operatorname{argmin}_T \left( \frac{1}{2\sigma^2} \sum_{i=1}^n \|y_{pi} - T(x_{pi})\|_2^2 - k \sum_{i=1}^n y_{ni}^T R x_{ni} \right)$$

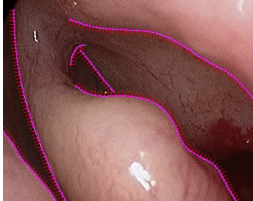

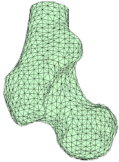
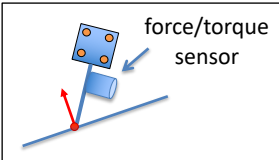
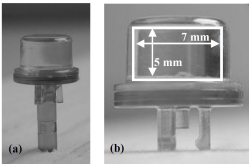
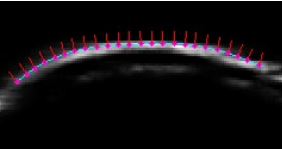
S. Billings and R. H. Taylor, "Iterative Most Likely Oriented Point Registration", in *Medical Image Computing and Computer-Assisted Interventions (MICCAI)*, Boston, October, 2014.

Copyright 2021 R. H. Taylor Engineering Research Center for Computer Integrated Surgical Systems and Technology

71



### Sources of Orientation Data

|   |   |   |
|---|---|---|
| <b>Video</b>  | <b>X-Ray</b>  | <b>Shape Models</b>   |
|  |  |  |
| <b>Tracked Pointer</b>  | <b>Oriented Fiducials</b>   | <b>Ultrasound</b>   |
|  |  |   |

Figures: [http://www.infodiv.com/wp-content/uploads/2013/09/level\\_registration1.png](http://www.infodiv.com/wp-content/uploads/2013/09/level_registration1.png); The Essential Physics of Medical Imaging, 3<sup>rd</sup> ed.; [http://www.infotech.edu/wp-content/uploads/2013/01/1\\_A\\_B\\_Cook-At-Gaby-3D-Ultrasound-Tests-Ultrasound-Technicians-by-300x225.jpg](http://www.infotech.edu/wp-content/uploads/2013/01/1_A_B_Cook-At-Gaby-3D-Ultrasound-Tests-Ultrasound-Technicians-by-300x225.jpg); [http://2001.allimg.com/photo/v0/105832128/CT\\_Scan\\_equipment.jpg](http://2001.allimg.com/photo/v0/105832128/CT_Scan_equipment.jpg); <http://goodsvolleyey.com/dl/?i=835588>; Liu X, Cevikalp H, Fitzpatrick JM (2003) Marker orientation in fiducial registration. In: Sonka M, Fitzpatrick JM, editors. SPIE, Medical Imaging 2003: Image Processing, Vol. 5032, pp. 1176–1185.

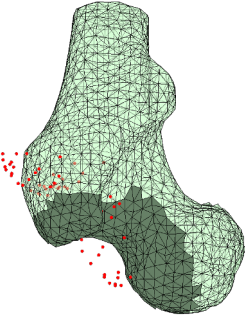
Copyright 2021 R. H. Taylor Credit: Seth Billing Engineering Research Center for Computer Integrated Surgical Systems and Technology

72

### Experiments

Performance comparison of IMLOP vs. ICP was made through a simulation study using a human femur surface mesh segmented from CT imaging.

- source shape created by randomly sampling points from the mesh surface (10, 20, 35, 50, 75, and 100 points tested)
- Gaussian [wrapped Gaussian] noise added to the source points (0, 0.5, 1.0, and 2.0 mm [degrees] tested)
- Applied random misalignment of [10,20] mm / degrees
- 300 trials performed for each sample size / noise level
- Registration accuracy (TRE) evaluated using 100 validation points randomly sampled from the mesh
- Registration failures automatically detected using threshold on final residual match errors



Example source point cloud sampled from dark region of target mesh.

ICP: threshold on position residuals only

IMLOP: threshold on position & orientation residuals

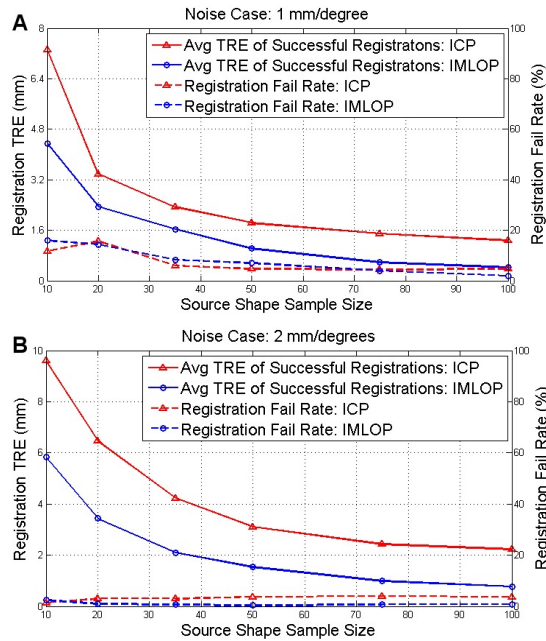
S. Billings and R. H. Taylor, "Iterative Most Likely Oriented Point Registration", in *Medical Image Computing and Computer-Assisted Interventions (MICCAI)*, Boston, October, 2014.

Copyright 2021 R. H. Taylor Engineering Research Center for Computer Integrated Surgical Systems and Technology

74

Average TRE of successful registrations and registration failure rates across all sample sizes for noise levels of 1 (A) and 2 (B) mm [degrees].

Registration failure threshold set to twice the noise level for both position and orientation.



S. Billings and R. H. Taylor, "Iterative Most Likely Oriented Point Registration", in *Medical Image Computing and Computer-Assisted Interventions (MICCAI)*, Boston, October, 2014. (accepted).

Copyright 2021 R. H. Taylor

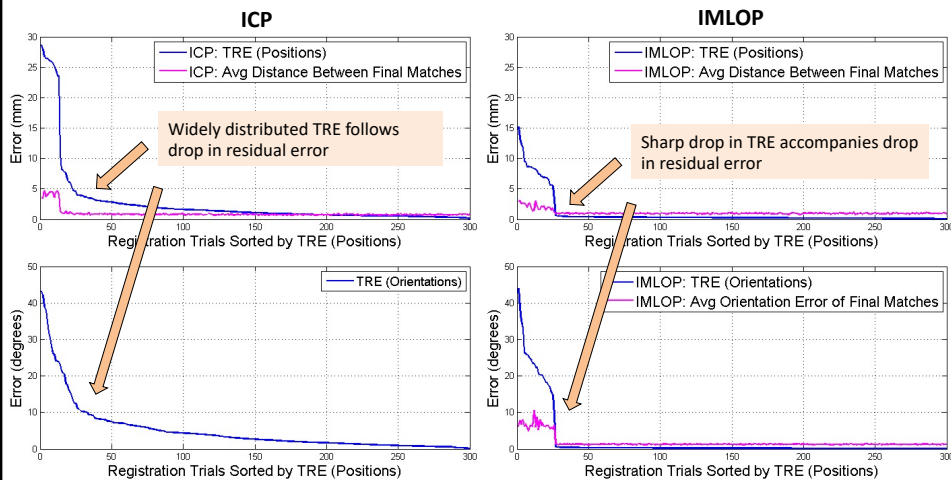
Engineering Research Center for Computer Integrated Surgical Systems and Technology



75

### Experiments

Results from 300 trials within a single sample size (75 points) and noise level (1.0 mm [degree]). NOTE: improved accuracy and failure detection capability for IMLOP.



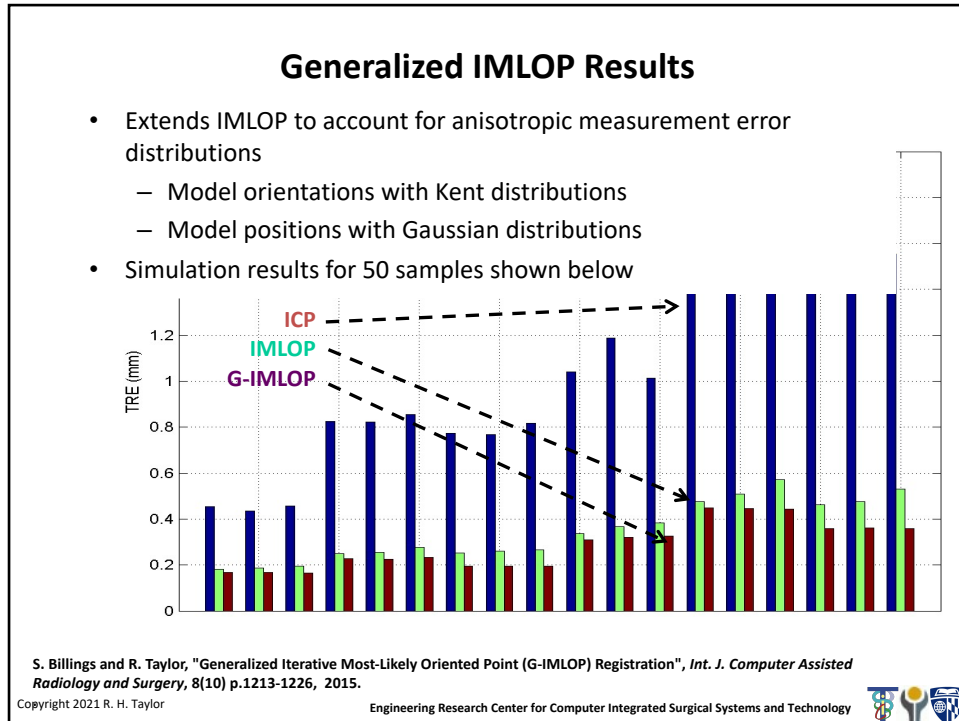
S. Billings and R. H. Taylor, "Iterative Most Likely Oriented Point Registration", in *Medical Image Computing and Computer-Assisted Interventions (MICCAI)*, Boston, October, 2014. (accepted).

Copyright 2021 R. H. Taylor

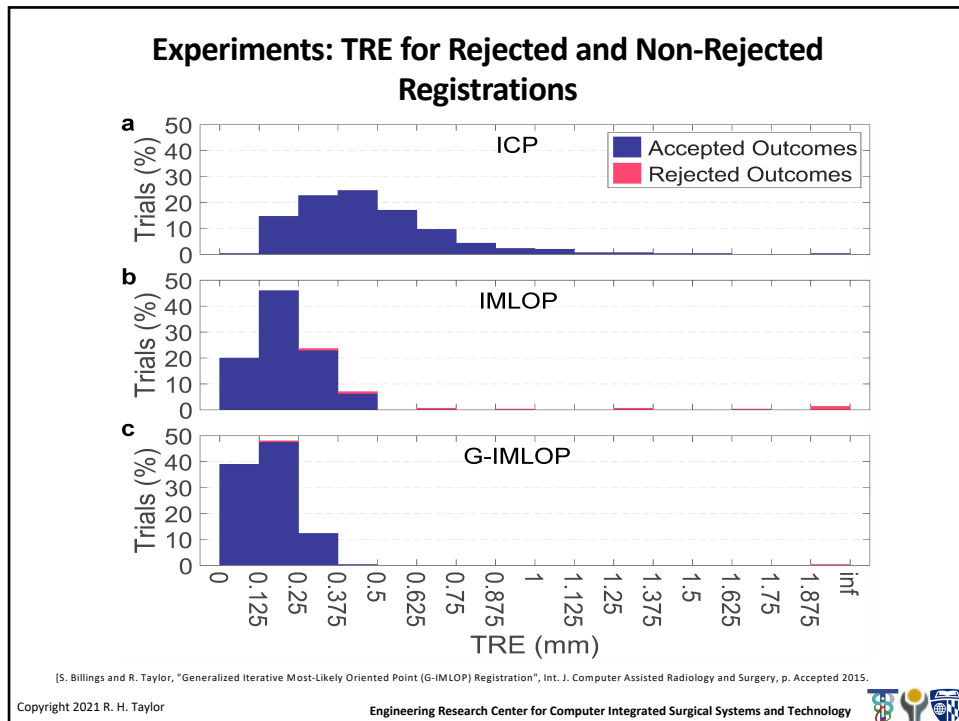
Engineering Research Center for Computer Integrated Surgical Systems and Technology



76



77



78

### Ultrasound-assisted Registration

(1) Generate surface model from CT

(2) Digitize proximal bone using tracked pointer

(3) Collect tracked US images of distal bone

(4) Register points/contours to surface model

S. Billings, H. J. Kang, A. Cheng, E. Boctor, P. Kazanzides, and R. Taylor, "Minimally invasive registration for computer-assisted orthopedic surgery: combining tracked ultrasound and bone surface points via the P-IMLOP algorithm", Int. J. Computer Assisted Radiology and Surgery, p. (epub ahead of print), 2015. <http://dx.doi.org/10.1007/s11548-015-1188-z> DOI 10.1007/s11548-015-1188-z

Copyright 2021 R. H. Taylor

Engineering Research Center for Computer Integrated Surgical Systems and Technology

79

### Intensity-based methods

Image 1

Image 2

$\Theta(\rho, \cdot)$

$\Theta(\rho, \text{Image 2})$

$E(\cdot, \cdot)$

Optimization Process

$\rho^* = \text{argmin } E(\text{Im 1}, \Theta(\rho, \text{Im 2}))$

$\rho^*$

Copyright 2021 R. H. Taylor

Engineering Research Center for Computer Integrated Surgical Systems and Technology

80

## Intensity-based methods

- Typically performed between images
- The “features” in this case are the intensities associated with pixels (2D) or voxels (3D) in the images.
- General framework:

$$\vec{\rho}^* = \min_{\vec{\rho}} E \left( Image_1, \Theta \left( \vec{\rho}, Image_2 \right) \right)$$

- Methods differ mostly in choice of transformation function  $\Theta(\cdot)$  and Energy function  $E(\cdot, \cdot)$ ,

Copyright 2021 R. H. Taylor

Engineering Research Center for Computer Integrated Surgical Systems and Technology



81

## Typical energy functions (not an exhaustive list)

### Normalized image subtraction

$$E(\text{Im}_1, \text{Im}_2) = \sum_{\vec{k}} \frac{|\text{Im}_1[\vec{k}] - \text{Im}_2[\vec{k}]|}{\max_j (|\text{Im}_1[\vec{j}] - \text{Im}_2[\vec{j}]|)}$$

### Normalized cross correlation (NCC)

$$E(\text{Im}_1, \text{Im}_2) = \frac{\sum_{\vec{k}} (\text{Im}_1[\vec{k}] - \text{avg}(\text{Im}_1)) (\text{Im}_2[\vec{k}] - \text{avg}(\text{Im}_2))}{\sqrt{\sum_{\vec{k}} (\text{Im}_1[\vec{k}] - \text{avg}(\text{Im}_1))^2} \sqrt{\sum_{\vec{k}} (\text{Im}_2[\vec{k}] - \text{avg}(\text{Im}_2))^2}}$$

### Mutual information

$$\rightarrow E(\text{Im}_1, \text{Im}_2) = \sum_{p \in \text{Im}_1, q \in \text{Im}_2} \Pr(p, q) \log \Pr(p, q) - \Pr_{\text{Im}_1}(p) \log \Pr_{\text{Im}_1}(p) - \Pr_{\text{Im}_2}(q) \log \Pr_{\text{Im}_2}(q)$$

Copyright 2021 R. H. Taylor

Engineering Research Center for Computer Integrated Surgical Systems and Technology



82

## Mutual Information

- First proposed independently in 1995 by Collignon and Viola & Wells.
- Very widely practiced
- Is able to co-register images with very different sensor modalities so long as there is a stable relationship between intensities in one modality with those in another
- Many “flavors” and variations

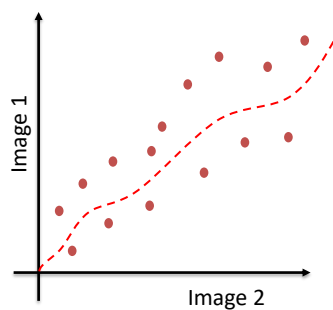
Copyright 2021 R. H. Taylor

Engineering Research Center for Computer Integrated Surgical Systems and Technology

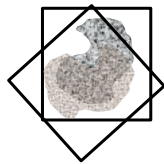


83

## Mutual Information



- The key idea is that the values of pixels in one image can predict the values of the pixels in the other image, even if the images come from different sensors
- The strength of this prediction will increase as the images become better aligned



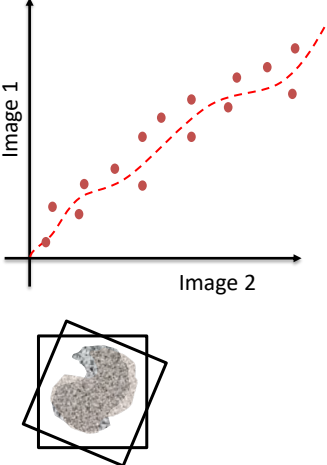
Copyright 2021 R. H. Taylor

Engineering Research Center for Computer Integrated Surgical Systems and Technology



84

### Mutual Information



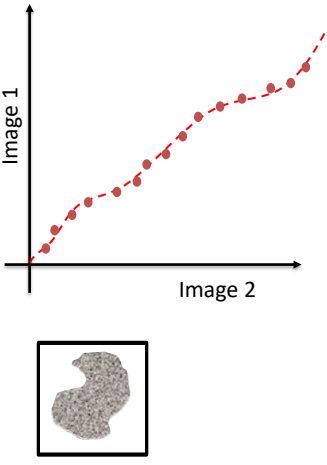
The figure shows a scatter plot with 'Image 1' on the vertical axis and 'Image 2' on the horizontal axis. Red dots represent data points, and a dashed red line indicates a positive correlation. Below the plot is a grayscale image of a kidney, which is tilted relative to a square frame, representing a misaligned image.

- The key idea is that the values of pixels in one image can predict the values of the pixels in the other image, even if the images come from different sensors
- The strength of this prediction will increase as the images become better aligned

Copyright 2021 R. H. Taylor Engineering Research Center for Computer Integrated Surgical Systems and Technology

85

### Mutual Information



The figure shows a scatter plot with 'Image 1' on the vertical axis and 'Image 2' on the horizontal axis. Red dots represent data points, and a dashed red line indicates a positive correlation. Below the plot is a grayscale image of a kidney, which is centered within a square frame, representing a better aligned image.

- The key idea is that the values of pixels in one image can predict the values of the pixels in the other image, even if the images come from different sensors
- The strength of this prediction will increase as the images become better aligned

Copyright 2021 R. H. Taylor Engineering Research Center for Computer Integrated Surgical Systems and Technology

86

## Mutual Information

### Entropy

$$H(a) = \Pr(a) \log \Pr(a)$$

$$H(a,b) = \Pr(a,b) \log \Pr(a,b)$$

### Mutual Information (Viola & Wells '95, Colligen '95)

$$\text{Similarity}(A,B) = H(A) + H(B) - H(A,B)$$

### Normalized mutual information (Maes et al. '97)

$$\text{Similarity}(A,B) = \frac{H(A) + H(B)}{H(A,B)}$$

### Objective function

$$E(\text{Im}_1, \text{Im}_2) = -\text{Similarity}(\text{Im}_1, \text{Im}_2)$$

Copyright 2021 R. H. Taylor

Engineering Research Center for Computer Integrated Surgical Systems and Technology

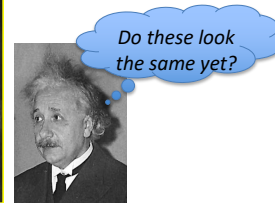
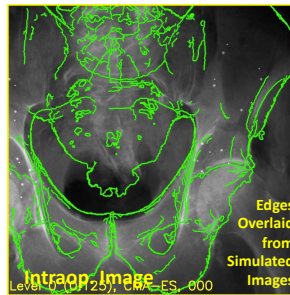


87

## Basic Idea of Intensity-Based 2D/3D Registration

- Assumes a pre-op CT is available
- Simulate many C-Arm images and choose the most similar to the intraoperative image
- Solves the following optimization problem:

$$\underset{\theta \in SE(3)}{\text{argmin}} \mathcal{S}(I_{\text{Intra-Op}}, \mathcal{P}(\theta, I_{\text{CT}}))$$



Slide credit: Robert Grupp

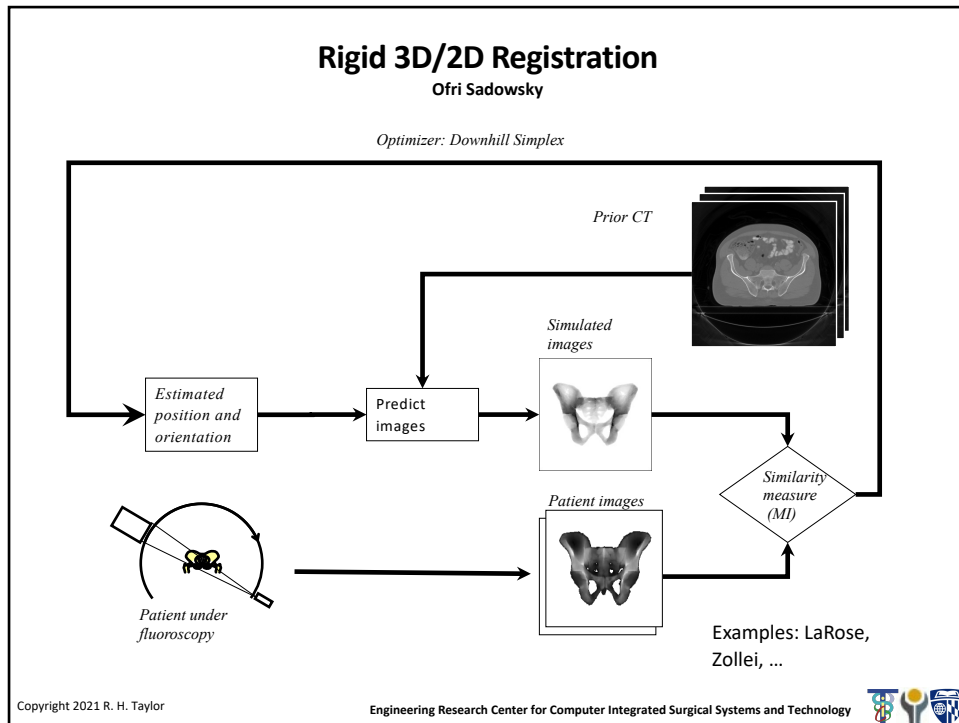
Copyright 2021 R. H. Taylor

Engineering Research Center for Computer Integrated Surgical Systems and Technology



88





89

ciis
BACS  
Biomechanical and Computer Integrated Surgical Systems Laboratory

## A clinical example (periacetabular osteotomy)

### Problem: Acetabular Dysplasia

Normal hip bones      Hip dysplasia

Image Source: ouh.nhs.uk

Dislocation Caused by Dysplasia

Image Source: James Heilman, MD

Slide credit: Robert Grupp

Copyright 2021 R. H. Taylor      Engineering Research Center for Computer Integrated Surgical Systems and Technology

91

**ciis** **BACS**  
Biomechanical and Integrated Surgical Systems Laboratory

### A clinical example (periacetabular osteotomy)

One Solution: Periacetabular Osteotomy (PAO)

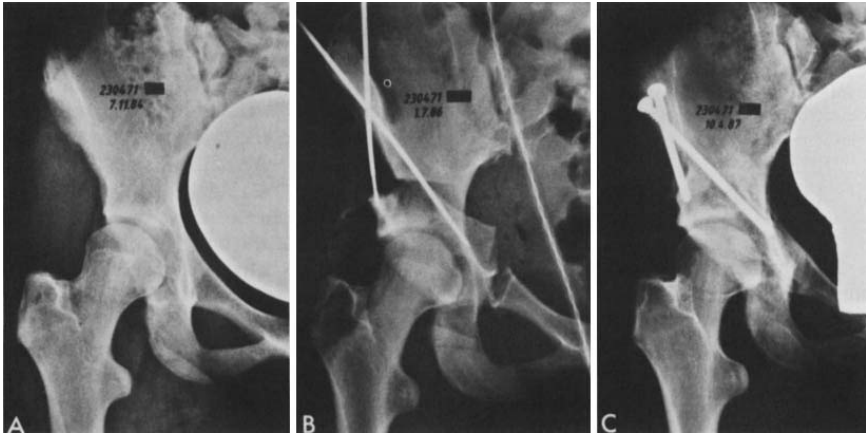


Image Source: Ganz 1988

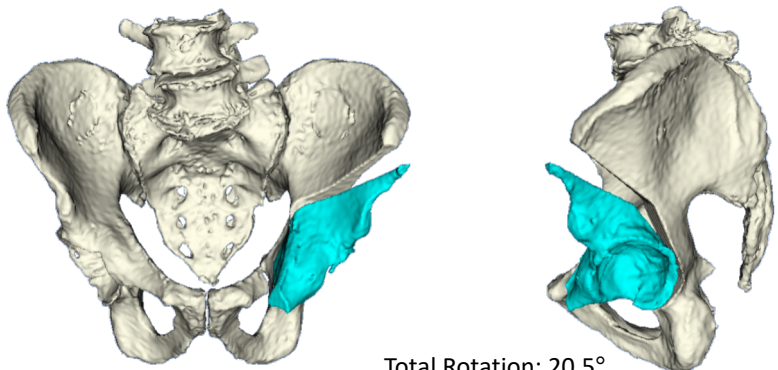
Copyright 2021 R. H. Taylor Slide credit: Robert Grupp Engineering Research Center for Computer Integrated Surgical Systems and Technology

92

**ciis** **BACS**  
Biomechanical and Integrated Surgical Systems Laboratory

### A clinical example (periacetabular osteotomy)

Goal: Automatic visualization and guidance



Total Rotation: 20.5°  
Anterior/Posterior Rotation: 3.7°  
Left/Right Rotation: 16.3°  
Inferior/Superior Rotation: 12.5°

Copyright 2021 R. H. Taylor Slide credit: Robert Grupp Engineering Research Center for Computer Integrated Surgical Systems and Technology

93

## Movement of the Osteotomy Fragment is Challenging



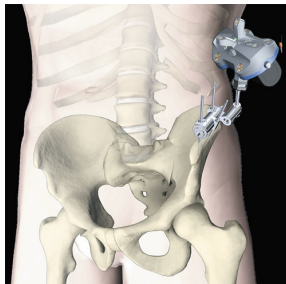
Copyright 2021 R. H. Taylor

Slide credit: Robert Grupp  
Engineering Research Center for Computer Integrated Surgical Systems and Technology

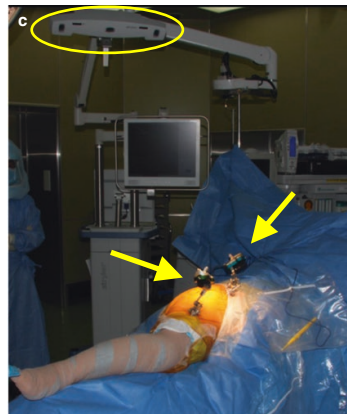


94

## One Approach for Computer-Assistance: Optical Tracking Devices



Source: Stiehl and Thornberry, 2016



Source: Sugano, CAOS for Hip and Knee, 2018

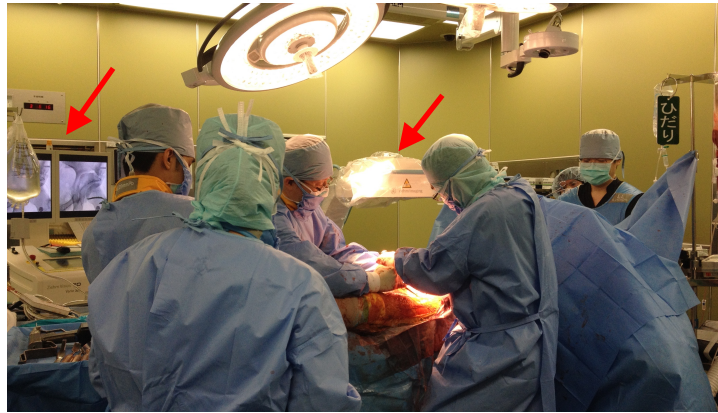
Copyright 2021 R. H. Taylor

Slide credit: Robert Grupp  
Engineering Research Center for Computer Integrated Surgical Systems and Technology



95

### Intraoperative Fluoroscopy is Available



Chapter 4: Pose Estimation Using Fluoroscopy

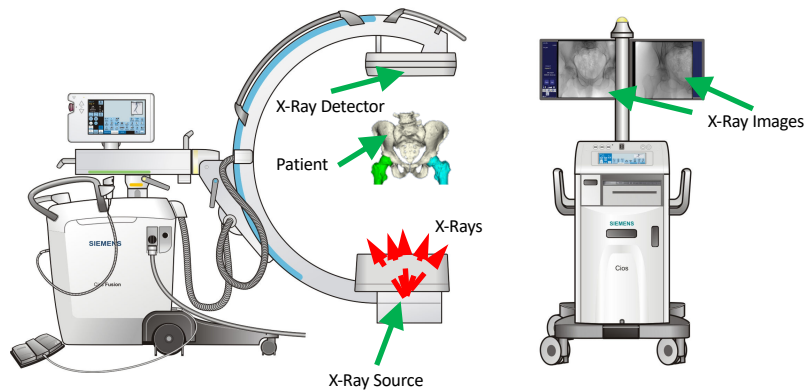
Copyright 2021 R. H. Taylor

Slide credit: Robert Grupp  
Engineering Research Center for Computer Integrated Surgical Systems and Technology



96

### Intraoperative X-Ray Imaging with Mobile C-Arm



C-Arm Image Source: Siemens CIOS Fusion Manual

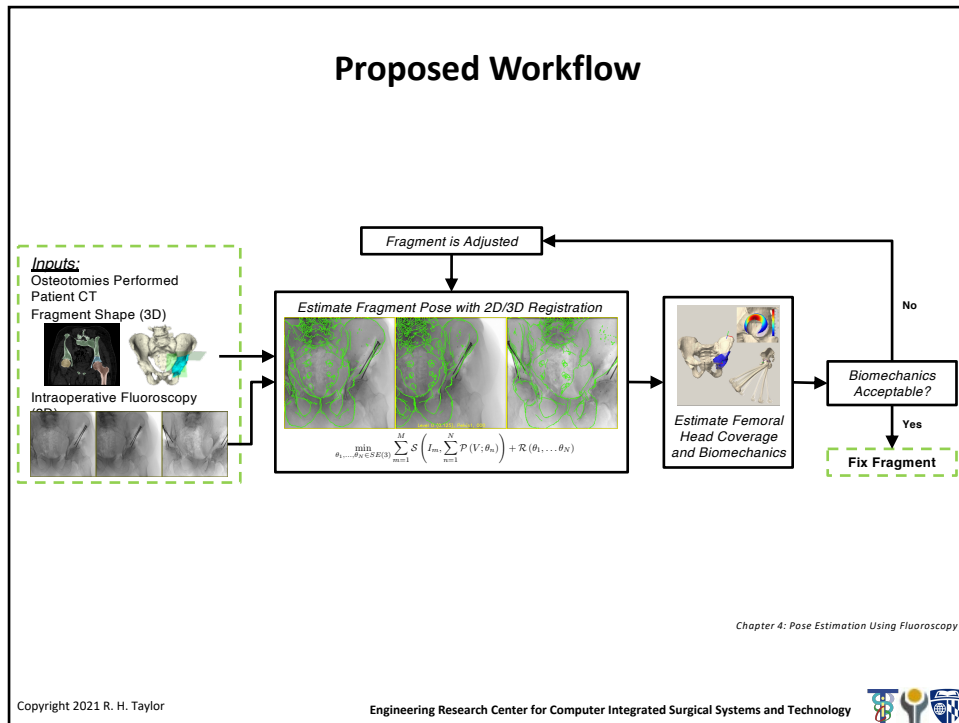
Chapter 4: Pose Estimation Using Fluoroscopy

Copyright 2021 R. H. Taylor

Slide credit: Robert Grupp  
Engineering Research Center for Computer Integrated Surgical Systems and Technology



97



98

ciis

### 3D-2D Registration of Osteotomy Fragments

$$\arg \min_{\theta_1, \dots, \theta_N \in SE(3)} \sum_{m=1}^M S \left( I_m, \sum_{n=1}^N P_m(ICT; \theta_n) \right)$$


Fixed Images  
with Moving  
Image Edges

Moving Images


R. Grupp, R. Murphy, M. Armand, R. Taylor

Copyright 2021 R. H. Taylor      Slide credit: Robert Grupp      Engineering Research Center for Computer Integrated Surgical Systems and Technology

99



### 3D-2D Registration of Osteotomy Fragments

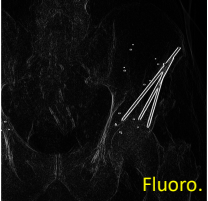


- Compute the Sobel derivatives in the X and Y directions of the two input images:


$$\nabla_X I_1, \nabla_X I_2, \nabla_Y I_1, \nabla_Y I_2$$

- Compute NCC between the corresponding gradient images:

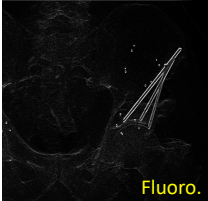
$$S(I_1, I_2) = NCC(\nabla_X I_1, \nabla_X I_2) + NCC(\nabla_Y I_1, \nabla_Y I_2)$$




$\nabla_X I_1$



$\nabla_X I_2$




$\nabla_Y I_1$



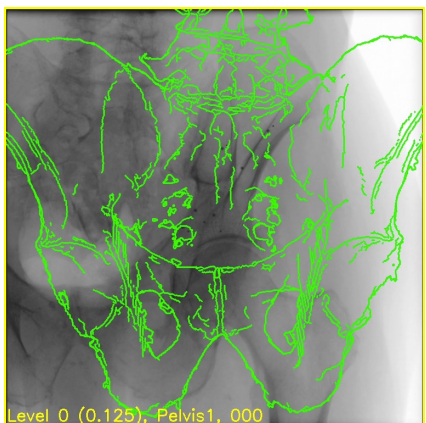
$\nabla_Y I_2$

R. Grupp, R. Murphy, M. Armand, R. Taylor

Copyright 2021 R. H. Taylor
Slide credit: Robert Grupp
Engineering Research Center for Computer Integrated Surgical Systems and Technology



100

### Initialize Using a Nominal AP View?

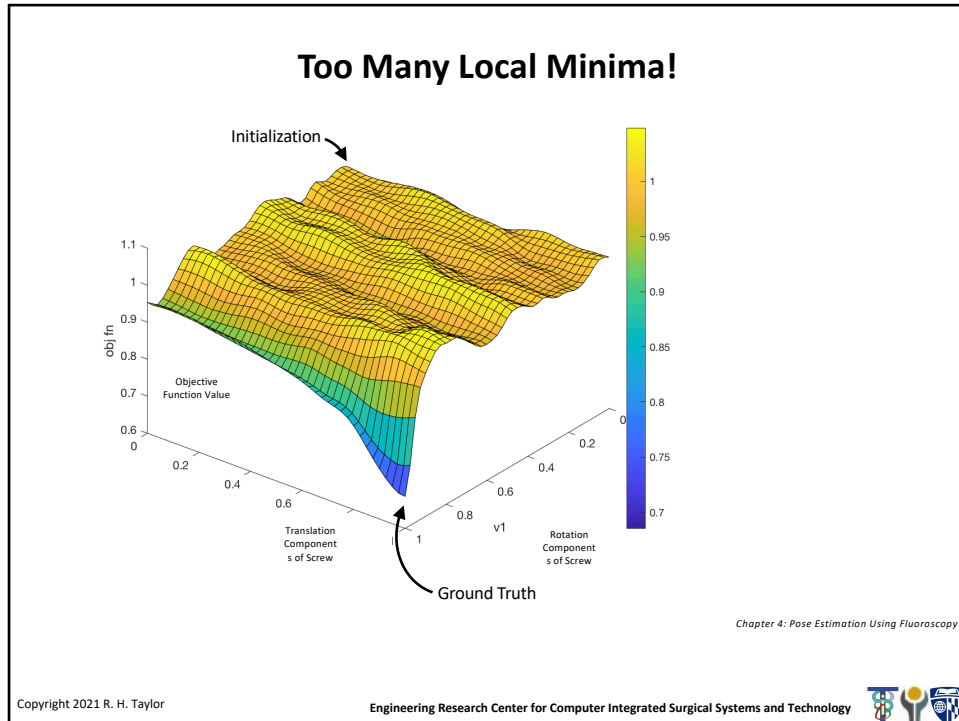


Level 0 (0.125), Pelvis1, 000

Chapter 4: Pose Estimation Using Fluoroscopy

Copyright 2021 R. H. Taylor
Slide credit: Robert Grupp
Engineering Research Center for Computer Integrated Surgical Systems and Technology


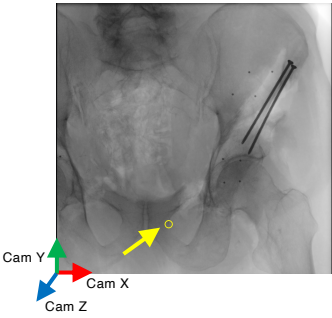
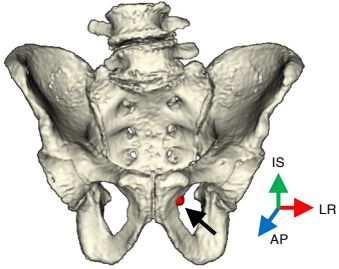
101



102

### Use a Single Landmark to Initialize Registration

- Assume the pelvis is in an AP orientation – this may be computed preoperatively
- Manually annotate a single landmark to recover translation

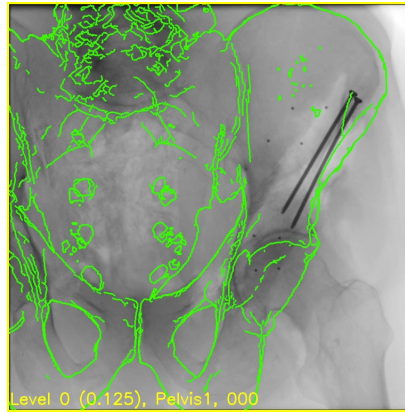



*Chapter 4: Pose Estimation Using Fluoroscopy*

Copyright 2021 R. H. Taylor      Slide credit: Robert Grupp      Engineering Research Center for Computer Integrated Surgical Systems and Technology

103

### Example of a Single Landmark Initialization



Chapter 4: Pose Estimation Using Fluoroscopy

Copyright 2021 R. H. Taylor

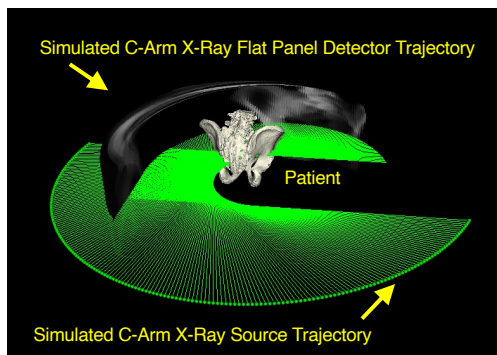
Slide credit: Robert Grupp  
Engineering Research Center for Computer Integrated Surgical Systems and Technology



104

### Automatically Initialize Second and Third Views

- Constrain C-arm motion to orbital rotation
- Perform an exhaustive search over  $\pm 90^\circ$  in  $1^\circ$  increments



Chapter 4: Pose Estimation Using Fluoroscopy

Copyright 2021 R. H. Taylor

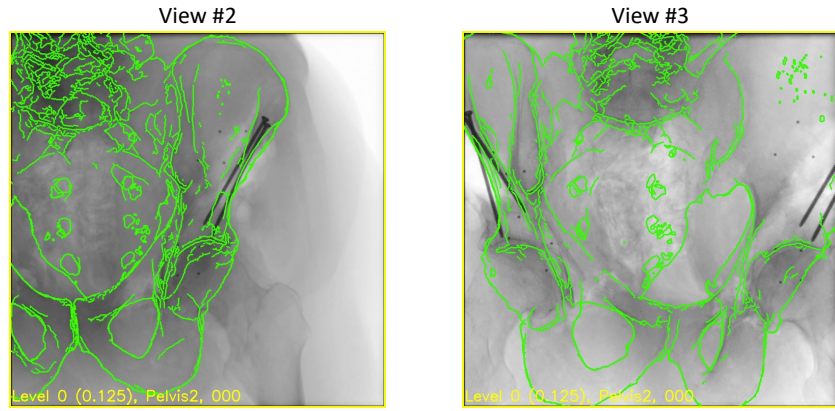
Slide credit: Robert Grupp  
Engineering Research Center for Computer Integrated Surgical Systems and Technology



105



### Example Initializations From Orbital Search



Chapter 4: Pose Estimation Using Fluoroscopy

Copyright 2021 R. H. Taylor

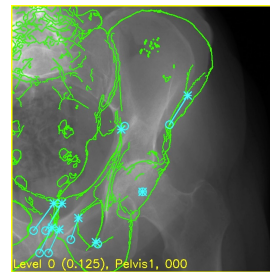
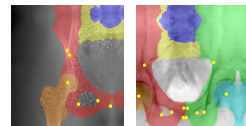
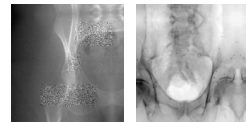
Slide credit: Robert Grupp  
Engineering Research Center for Computer Integrated Surgical Systems and Technology



106

### Automatic Landmark-Based Initialization

- Train a CNN to recognize approximate landmark positions in x-ray images
- Use landmark-based 2D-3D registration to initialize registration
- Combine landmark and intensity objective functions
- Use segmentation labels to ignore intensities of irrelevant anatomy



Copyright 2021 R. H. Taylor

Images: Robert Grupp  
Engineering Research Center for Computer Integrated Surgical Systems and Technology



107

## Why Not Simultaneously Use Intensities and Features?

- Registration objective function:

$$\min_{\theta_P, \theta_{LF}, \theta_{RF} \in SE(3)} \lambda \mathcal{S}(\mathcal{P}(\theta_P, \theta_{LF}, \theta_{RF}), I) + (1 - \lambda) \mathcal{R}(\theta_P, \theta_{LF}, \theta_{RF})$$

Image Similarity Term
Regularization Term

- Usually, regularization penalizes the amount of rotation and translation away from initialization
- Why not directly include the landmark re-projection as regularization?

$$\mathcal{R}(\theta_P) = \frac{1}{2\sigma_l^2} \sum_{l=1}^{N_l} \left\| \mathcal{P}(p_{3D}^{(l)}; \theta_P) - p_{2D}^{(l)} \right\|_2^2$$

- Can also think of this as running landmark registration and regularizing on image appearance

Chapter 6: Automatic and Robust Registration

Copyright 2021 R. H. Taylor

Slide credit: Robert Grupp

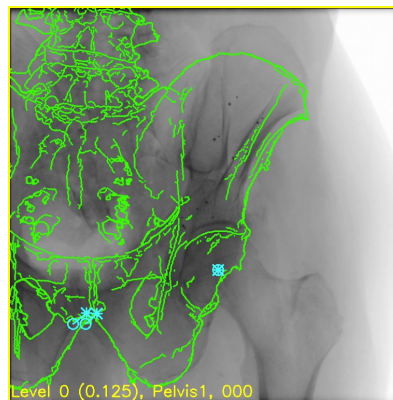
Engineering Research Center for Computer Integrated Surgical Systems and Technology



108

## Include Landmark Reprojection Into Objective Function

- Landmarks Detected in 2D are Shown as Cyan Circles
- Landmarks Projected from 3D are Shown as Cyan Asterisks \*
- Cyan Lines Indicate Correspondence
- The Initial Pose Aligns the 2D and 3D Left Femoral Head Centers



Chapter 6: Automatic and Robust Registration

Copyright 2021 R. H. Taylor

Engineering Research Center for Computer Integrated Surgical Systems and Technology



109

